Laser-induced fluorescence detection in high-throughput screening of heterogeneous catalysts and single cells analysis

by

Hui Su

A dissertation submitted to the graduate faculty

in partial fulfillment of the requirements for the degree of

DOCTOR OF PHILOSOPHY

Major: Analytical Chemistry

Major Professor: Edward S. Yeung

Iowa State University

Ames, Iowa

2001

Graduate College

Iowa State University

This is to certify that the Doctoral dissertation of

Hui Su

has met the dissertation requirements of Iowa State University

Major Professor

For the Major Program

For the Graduate College

To my mother

TABLE OF CONTENTS

ABSTRACT ..... **vi**

GENERAL INTRODUCTION **1**

Dissertation Organization *1*

PART 1. HIGH-THROUGHPUT SCREENING OF HETEROGENEOUS CATALYSTS **3**

CHAPTER 1. INTROUDUCTION **4**

Combinatorial Chemistry in Solid-State Materials Discovery *4*

High Throughput Screening of Heterogeneous Catalysts *7*

My Goal *13*

References *13*

CHAPTER 2. HIGH-THROUGHPUT SCREENING OF HETEROGENEOUS CATALYSTS BY LASER-INDUCED FLUORESCENCE IMAGING **23**

Acknowledgement *27*

References *27*

CHAPTER 3. COMBINATORIAL SCREENING OF HETEROGENEOUS CATALYSTS IN SELECTIVE OXIDATION OF NAPHTHALENE BY LASER-INDUCED FLUORESCENCE IMAGING **34**

Abstract *34*

Introduction *35*

Experimental Section *37*

Results and Discussion *42*

Conclusion *48*

Acknowledgement *49*

References *50*

CHAPTER 4. COMBINATORIAL STUDY OF ZEOLITE IN CATALYZING ACYLATION OF BENZEN VIA LASER-INDUCED FLUORESCENCE IMAGING 67

Abstract *67*

Introduction *68*

Experimental Section *70*

Results and Discussion *72*

Conclusion *75*

Acknowledgement *75*

References *76*

PART 2. STUDY OF SINGLE CELL DEGRANULATION 89

CHAPTER 5. STUDY OF CELL DEGRANULATION WITH SIMULTANEOUS MICROSCOPE IMAGING AND CAPILLARY ELECTROPHORESIS 90

Abstract *90*

Introduction *90*

Experimental Section *92*

Results and Discussion *94*

Conclusions *98*

Acknowledgement *98*

References *99*

CHAPTER 6. CONCLUSIONS 104

APPENDIX. SUPPORTING INFORMATION 105

ACKNOWLEDGMENTS 117

ABSTRACT

Laser-induced fluorescence detection is one of the most sensitive detection techniques and it has found enormous applications in various areas. The purpose of this research was to develop detection approaches based on laser-induced fluorescence detection in two different areas, heterogeneous catalysts screening and single cell study.

First, we introduced laser-induced imaging (LIFI) as a high-throughput screening technique for heterogeneous catalysts to explore the use of this high-throughput screening technique in discovery and study of various heterogeneous catalyst systems. This scheme is based on the fact that the creation or the destruction of chemical bonds alters the fluorescence properties of suitably designed molecules. By irradiating the region immediately above the catalytic surface with a laser, the fluorescence intensity of a selected product or reactant can be imaged by a charge-coupled device (CCD) camera to follow the catalytic activity as a function of time and space. By screening the catalytic activity of vanadium pentoxide catalysts in oxidation of naphthalene, we demonstrated LIFI has good detection performance and the spatial and temporal resolution needed for high-throughput screening of heterogeneous catalysts. The sample packing density can reach up to 250 ×250 subunits/cm^2 for 40-μm wells. This experimental set-up also can screen solid catalysts via near infrared thermography detection.

We further applied the LIFI screening system for combinatorial discovery of heterogeneous catalysts and reaction condition optimization for naphthalene oxidation, as well as combinatorial study of catalytic performance of zeolites in acylation of aromatics. For combinatorial discovery of heterogeneous catalysts for naphthalene oxidation, we tested the catalytic performance of libraries of various combinations of binary and ternary vanadium-

based catalysts; some combinations with much better catalytic performance than pure vanadium pentoxide were discovered. Sample preparation methods and reaction temperatures were screened for optimization of catalytic performance. Combined information obtained by the fluorescence and infrared screening, promotion effects of different oxides, Mo (VI), Sn (V), Ti (V) and W (VI), were revealed in a high-throughput fashion. I also introduced LA-ICP-MS as a high-throughput composition analysis technique for solid-state libraries. In a combinatorial study of the catalytic performance of zeolites in acylation of aromatics, the effect of temperature, Si/Al ratios and the structure of zeolites on their catalytic performance were studied by in situ monitoring the catalytic reactions by laser-induced fluorescence imaging screening technique.

In the second part of this dissertation, I used laser-induced native fluorescence coupled with capillary electrophoresis (LINF-CE) and microscope imaging to study the single cell degranulation. On the basis of good temporal correlation with events observed through an optical microscope, we have identified individual peaks in the fluorescence electropherograms as serotonin released from the granular core on contact with the surrounding fluid.

GENERAL INTRODUCTION

Dissertation Organization

This dissertation consists of two parts starting with a general introduction. Chapter two in part 1 and chapter 5 in part 2 are published scientific manuscripts. Chapter 3 and chapter 4 in part 1 are manuscripts prepared for publication. General conclusions summarize the work and provide some prospective for future research. Appendices include the supporting materials.

Part 1. High-throughput Screening for Heterogeneous Catalysts

In effort of discovery new materials with useful properties, combinatorial chemistry has established itself as one of the most important methodology, which is capable of fastening the discovery process in hundreds and thousands times. The application of combinatorial chemistry in solid-state heterogeneous catalysis is a relatively young research area compared with its application in pharmaceutical industry. There are three aspects of equal importance in solid-state combinatorial chemistry differing from organic combinatorial chemistry: 1) combinatorial synthesis, 2) high-throughput screening, and 3) effective composition analysis of library components. Success has been achieved in combinatorial synthesis of solid-state catalysts library by thin-film deposition and liquid dosing techniques, and more effort is needed in developing high-throughput screening techniques for heterogeneous catalysts as well as fast and effective approach for composition analysis of solid catalysts on the libraries. In part 1 of this dissertation I described the development of a high-throughput screening technique for heterogeneous catalysts by laser-induced fluorescence imaging. I also demonstrated its applications in combinatorial discovery of

active catalysts for catalytic oxidation of aromatics, and combinatorial study of catalytic properties of zeolites in acylation of aromatics.

Part 2. Study of Single Cell Degranulation

The cell is the fundamental unit of life. Studying the chemistry of dynamic cellular processes should allow us to better understand cellular functions. In this work, I studied the cell degranulation with simultaneous microscope imaging and capillary electrophoresis (CE). A high-resolution charged-coupled device (CCD) microscope system was used to monitor a degranulating mast cell trapped inside a capillary column. After a well-defined time delay, the released serotonin, one of the granular products, was detected with laser-induced fluorescence-CE. Therefore we were able to follow an exocytotic event with unprecedented detail.

PART 1. HIGH-THROUGHPUT SCREENING OF HETEROGENEOUS CATALYSTS

CHAPTER 1. INTROUDUCTION

Combinatorial Chemistry in Solid-State Materials Discovery

Overview

A new discovery is always exciting, but the cost of time and resources is not. The traditional approach of discovery is a one-by-one strategy: synthesize a new material with one formula, and then test this material for certain property, again and again, until one formula is found with the desired property. Nowadays, this slow-pace process of discovery can no longer satisfy people's needs of new materials. Numerous efforts have been devoted to accelerate the discovery of new materials, and combinatorial chemistry is the most focused and successful approach. An ideal combinatorial solution of discovery is to identify the target compound(s) by simultaneously testing the specific property of a large number of compounds with different formulas, which were synthesized at the same time. The realization of combinatorial methodology can make the discovery process hundreds, even thousands, of times more efficient. The concept of combinatorial chemistry can be traced back to 1963 with R. B. Merrifield's solid-state synthesis of peptides, [1] and it has achieved enormous success in drug discovery. But, the impact of combinatorial chemistry is much more than that. The combinatorial discovery in solid-state materials and its applications outside the pharmaceutical industry came much later, but its future is as promising as it is in drug discovery because solid-state materials with useful properties, such as superconductors, magnetic materials, light emitting materials, and catalysts, can benefit human society and have huge economical potential.

The Forerunner: "Multiple- Sample Concept"

In 1970, Joseph J. Hanak brought up a new concept of material research, the "Multiple-sample concept", after he became increasingly impatient with the traditional methodology of material research.[2] Hanak introduced an approach that consisted of synthesizing, analyzing, testing, and evaluating of multi-component systems in single steps. A radio-frequency co-sputtering technique was adopted and modified to co-deposit two or three elements on a substrate to provide a continuum of compositions; then, the compositions were determined by computing the thickness of a few spots on the sputtered thin film. Many new superconductors were found with this approach.[3] Hanak's approach resulted in up to a hundred-fold increase in the rate of discovering new materials.

Hanak's idea was the forerunner of a concept that is now taking material science by storm: combinatorial approach. But his idea never became popular because of the lack of computers in the 1970s: the compositional analysis, automated testing and data processing can't be fulfilled without a computer.

First Success: Thin Film Deposition

More than 20 years after Hanak's " Multiple-Sample Concept", inspired by the success of combinatorial chemistry in biology, material scientists once again questioned the traditional approach of materials discovery with much more sophisticated modern technologies. Peter G. Schultz and Xiaodong Xiang in Lawrence Berkeley National Laboratory (LBNL) decided to extend the success of combinatorial approach from organic and biological molecules to the remainder of the periodic table, and for the first time they

demonstrated that the combinatorial approach could be used to discover solid-state materials with novel properties.[4]

Schultz and his coworkers developed a methodology of thin film deposition, which allowed the parallel synthesis of spatially addressable arrays containing superconducting thin film. By sequentially depositing the individual precursors of interesting on suitable substrate through a series of physical masks, a spatially defined library of solid-thin films could be generated. In their study, polished MgO or $LaAlO_3$ single crystals were used as substrate, and CuO, Bi_2O_3, CaO, PbO, $SrCO_3$, Y_2O_3, and $BaCO_3$ were used as precursors to make superconductive cuprates. After a series of depositions, the library array was thermally processed to produce crystalline cuprates. Then, the resistance at each site in the array was measured as a function of temperature. The sites containing the known superconductors showed large resistance drops, which are indicative of superconductivity. Superconductivity was found in thin films containing $BiCuCaSrO_x$ and $BiPbCuCaSrO_x$ in a 16-member binary library, which agreed with what had been found by conventional one-at-a-time synthesis methods. Effects of deposition sequence and elemental composition were evaluated in a 128-member library.

The work of Xiang and Shultz showed that relatively complex solid-state materials with useful property could be made and found in a parallel fashion, and the discovery process could be accelerated by a factor of thousands. Soon, other reports began appearing in the literature, using combinatorial methods to search for a wide variety of materials including magnetoresistive materials,[5] luminescent materials,[6-9] and catalysts.[10-13]

Solution-Phase Synthesis of Solid-State Materials Libraries

Thin film deposition has achieved stunning success in combinatorial discovery of solid-state materials; however, it faces the upgrading problem of the bulk synthesis of newly discovered compounds. In addition, for many materials, solid-state synthesis may not be best accomplished by thin film deposition. The solution-phase synthesis such as sol-gel and hydrothermal synthesis, polymerization, and precipitation reaction is free of the above problems. With the combination of solution-phase synthesis and automated ink-jet dosing system, a micro-scale library of new luminescent materials was prepared from aqueous solutions of La, Eu, Gd, and Al nitrates by Xiao-dong Sun and his coworkers. [14] The volumes as small as 0.5nL could be dosed with high precision and spatial resolution. Similar ink-jet technique was also applied in the first combinatorial discovery of a new heterogeneous electrocatalysts for applications in the fuel cell, [12] Mellouk et al projected 3-dimensional phase diagrams of Pt, Os, Rh, Pd, and Ir onto planar libraries and investigated the activity of the components for methanol decomposition by use of a H^+ -sensitive fluorescence indicator.

High Throughput Screening of Heterogeneous Catalysts

Overview

Thin film deposition and ink-jet liquid dosing techniques allow us to rapidly synthesize a large number of solid-state materials. However, that is just the first step in combinatorial discovery of solid-state materials. A high throughput screening technique is highly desired to test the properties of individual materials in a solid-state library. For solid-state materials, such as luminescent materials, superconductors, and magnetoresistive

materials, fast screening does not seem to be a problem since only the specific properties of the solid materials are accessed: superconductivity and magnetoresistivity can be tested by scanning probes, and luminescence can even be tested by human eyes. For solid heterogeneous catalysts, the situation is totally different: people are interested in their ability to interact with other compounds, and catalytic activity is the screening target. Most of the heterogeneous catalytic reactions are in gas phase, which makes high throughput screening of heterogeneous catalysts even more difficult.

A search for catalysts using combinatorial approach has been underway for several years, scientists have devised several methods for screening solid catalysts libraries, and each has its own advantages and disadvantages.

IR Thermography

R. C. Willson and his coworker in 1996 reported infrared thermographic screening of combinatorial libraries of heterogeneous catalysts, which was the first example of a highly parallel approach to catalyst screening of heterogeneous oxidation catalysts. [15] Given that catalytic reactions are exothermic, active catalysts reveal themselves as "hot spots" in infrared images, which is the screening base of IR thermography. Catalysts on the solid-state library can be tested simultaneously and in situ by this screening technique. In Willson's study, combinatorial screening of catalysts for hydrogen oxidation was described. The catalysts were placed in a reactor in predefined locations; then, they were scanned with a IR imaging camera having a temperature sensitivity of 0.025°C (figure 1). Initial measurements of IR emission were made in the absence of reaction. Ir, Pd, and Pt were found to be

catalytically active in this reaction starting at 80°C whereas the other candidates remained inactive up to 300 °C.

IR thermography also was applied to the screening of potential heterogeneous catalysts by Wilhelm F. Maier et al.[16] They examined different compositions of amorphous microporous mixed-metal oxides based on silica and titania. Microliter amounts of precursor solutions were pipetted into tiny wells on the surface of a slate substrate; then, the solutions were thermally processed to yield an array of solid samples. In their study, Maier and coworkers assessed a library of 37 oxides for catalytic activity in the hydrogenation of 1-hexyne at 100°C. An IR image taken during the reaction revealed four spots that were hotter than the substrate, indicating that these samples were active catalysts in the reaction.

These studies have proven that thermal imaging can provide convenient and fast parallel testing of whole catalyst libraries. However, no chemical information about the products generated in the reaction can be obtained because only the temperature is measured. IR thermography can tell which catalyst is active, but can't tell for which reaction the catalyst is active. Absence of chemical information is the major limitation of thermal imaging screening technique since there is more than one reaction involved in most of the catalytic heterogeneous reaction.

Laser-induced Resonance-enhanced Multiphoton Ionization

Selim M. Senkan described a laser-based high throughput screening method for solid-state catalysts that activates the dehydrogenation of cyclohexane to benzene. [17] In Sekan's work, a tunable laser was used for the selective photoionization of product molecules in the vicinity of catalytic sites, and then the resulting photoions or photoelectrons were detected by

an array of microelectrodes. The cross-section of ionization is significantly enhanced only when the laser frequency is tuned to a real intermediate electronic state of a molecule, which means that simultaneous photoionization of the reactants and other products can be avoided. To demonstrate this principle, Senkan constructed an 8×9 library containing Pt and Pa catalysts (figure2(a)). Reactant gases containing cyclohexane were forced through the individual sites, and a UV laser beam was passed through the air space above the sites (figure 2(b)). The beam was tuned to a wavelength that selectively ionized any benzene formed to C6H6+and an electron. These charged species were detected by an array of microelectrodes placed above the sites near the laser beam. The signals recorded in the experiment clearly distinguished between the active sites and the inactive sites on the catalyst library.

There are some limitations in Senkan's photonionization set up as a combinatorial screening technique. One-dimensional detection scheme has decided that the throughput of screening can not be very impressive; probing the ions in the reactor with microelectrodes is invasive and hard to use in real applications not to mention all the mirrors and electrodes involved in this set up. Senkan's original set up evolved to a microreactor array (figure 2(c)), which was used to screen a 66-member library of Pt-Pa-In compositions for catalytic activity in the cyclohexane dehydrogenation reaction. [18] The microreator array consists of 17 narrow micromachined channels that extend through a nonporous silica ceramic slab about 3 inches long. Each channel contains a small well for the catalyst pellet and a piece of porous alumina impregnated with 1% by weight of a Pt-Pd-In composition. The slab was heated to the reaction temperature while the reaction gas mixture was fed into each of the 17 channels in parallel. Near the exit, all 17 streams passed through the laser beam, which ionized the benzene product. The resulting benzene ions were picked up by an array of 17

microelectrodes. Each run of the microreactor array took 2 or 3 minutes. To screen the 66-member library, this procedure had to be repeated 5 times.

Laser-induced resonance-enhanced multiphoton ionization has proven to be able to screen the catalytic activities of multiple solid catalysts by identifying the products that emanate from each individual catalyst site on an array. However, the problems that existed in Senkan's original photonionization screening set up basically were not solved in the second model. The generality of this photonionization screening approach itself still remains unproven.

Scanning Microprobe Mass Spectrometry

Selectivity is a criterion that is as important as catalytic activity for heterogeneous catalysts. Scanning microprobe mass spectrometry has been developed into a high throughput screening technique for both catalytic activity and selectivity of solid catalysts by Symyx researchers (figure 3(a)). [13] It was used to screen libraries of Rh-Pd-Pt compositions for activity in reactions that occur in catalytic converters, such as $CO + 1/2O_2 \rightarrow CO_2$. In their work, 15×15×15 triangular libraries containing 120 different catalysts each were generated by RF sputtering thin film technique or liquid dosing robotics. A probe system of concentric tubes allows the gas stream containing the reactants (CO and O_2) to be delivered to a catalyst site and then removed by vacuum for analysis in a mass spectrometer (figure 3(b)). The 1.5-mm diameter catalyst site was heated to a desired temperature by a laser before the sampling was done. The 120-member library sat on a stage that automatically moved each catalyst sites into position under the probe. Each measurement was completed in about one minute, and only slightly more than two hours was needed to screen the entire library. The screening

results turned out that Rh and Rh rich compositins were most active for producing CO_2 in the three noble metals they tested. The catalytic performance of Cu replacement catalysts was evaluated by this system.

Shortly after Symxy's first report of the Scanning MS high throughput screening system, they announced a full implementation and integration of combinatorial methodologies for synthesis, screening, discovery, and optimization of multiple component catalysts for oxidative dehydrogenation of C_2H_6.[19] In addition to MS, photothermal deflection was developed as part of screening system (figure 3 (c)).

Scanning MS is capable of testing more than one product in screening the catalytic performance of heterogeneous catalysts. However, this is still a one by one testing system, which can not fundamentally improve the screening throughput.

Fluorescence Indicator

Mallouk and co-workers demonstrated that metal alloy electrocatalysts could be optimized by using the production of protons during the electrochemical oxidation of methanol in a fuel cell.[12] By converting the ions generated in an electrochemical reaction to a fluorescence signal, the active composition in a large electrode array was identified (figure 4). A fluorescence acid-base indicator was used to image high concentrations of hydrogen ions, which were generated in the electrooxidation of methanol. In a 645-member electrode array containing five elements, Pt, Ru, Os, Ir, and Rh, 80 binary, 280 ternary, and 280 quaternary combinations were screened to identify the most active regions of phase space. Subsequent " zoom" screens pinpointed several very active compositions.

Screening scheme based on fluorescence indicator can process a large number of catalyst combinations simultaneously with high accuracy, but its application limits in solution based heterogeneous catalytic reaction in which fluorescence-induced ions must be generated.

My Goal

Recently significant progress has been made in high-throughput screening of heterogeneous catalysts; however there is still a long way to go in developing sophisticated high-throughput screening techniques. Our goal is to develop an alternative to high-throughput screening technique of heterogeneous catalysts based laser-induced fluorescence imaging and to apply this technique in screening catalytic performance of different heterogeneous catalysts.

References

1. R. B. Merrifield, *J. Am. Chem. Soc.* 1963, 85, 2149
2. J. J. Hanak, *J. Mater. Sci.* 1970, 5, 964
3. J. J. Hanak; J. I. Gittleman; J. P. Pellicane and S. Bozowski, *Phys. Letters* 1969, 30A, 201
4. X. D. Xiang; X. Sun; G. Briceno; Y. Lou; K. A. Wang; H. Chang; W. G. Wallace-Freedman; S. W. Chen and P. G. Schultz, *Science* 1995, 268, 1738-1740
5. G. Briceno; H. Chang; X. D. Sun; P. G. Schultz; X. D. Xiang. *Science* 1995, 270, 273-275

6. E. Danielson; J. H. Golden; E. W. Mcfarland; C. M. Reaves; W. H. Weinberg and X. D. Wu, *Nature* 1997, 389, 944-948

7. T. Wei; W. G. Wallace-Freedman; P. G. Shultz and X. D. Xiang, *Apply. Phys. Lett.* 1998, 72, 525

8. E. Danielson; M. Devenny; D. M. Giaquinta; J. H. Golden; R. C. Haushalter; E. W. McFarland; D. M. Poojary; C. M. Reaves; W. H. Weinberg; X. D. Wu, *Science* 1998, 279, 837

9. J. Wang; Y. Yoo; C. Gao; I. Takuchi; X. Sun; H. Change; X. D. Xiang; P. G. Schultz, *Science* 1998, 279, 1712

10. S. J. Taylor; J. P. Morken. *Science* 1998, 280, 267-270

11. S. M. Senkan. *Nature* 1998, 394, 350-353

12. E. Reddington; A. Sapienza; B. Gurau; R. Viswanathan; S. Sarangapani; E. S. Smotkin and T. E. Mallouk, *Science* 1998, 280, 1735-1737

13. P. Cong; R. D. Doolen; Q. Fan; D. M. Giaquinta; S. Guan; E. W. Mcfarland; D. M Poojary; K. Self; H. W. Turner and W. H. Weinberg, *Angew. Chem. Int. Ed.* 1999, 38, 484-488

14. X. D. Sun; K. A. Wang; Y. Yoo; W. G. Wallace-Freedman; C. Gao; X. D. Xiang and P. G. Schultz, *Adv. Mater.* 1997, 9, 1046-1049

15. F. C. Moates; M. Somani; J. Annamalai; J. T. Richardson; D. Luss; R. C. Wilson. *Ind. Eng. Chem. Res.* 1996, 35, 4801-4803

16. J. Klein; K. W. Lehmann; H. W. Schmidt; W. F. Maier. *Angew. Chem. Int. Ed.* 1998, 37, 3369-3372

17. S. M. Senkan, *Nature* 1998, 394, 350-353

18. Selim M. Senkan and Sukru Ozturk, Angew. Chem. Int. Ed. 1999, 38, 791-795

19. P. J. Cong; A. Dehestani; R. Doolen; D. M. Giaquinta; S. Guan; V. Markov; D. Poojary; K. Self; H. Turner and W. H. Weinverg, *Proc. Nat. Acad. Soc.* 1999, 96, 11077-11080

FIGURE CAPTIONS

FIGURE 1. IR thermography screening of heterogeneous catalysts [15]

FIGURE 2. High throughput screening of catalysts libraries with laser-induced resonance-enhanced multiphoton ionization [17,18]

(a) Experimental set-up for the screening of 72-member catalysts library

(b) Design of individual sites on the catalyst library

(c) Array microreactor system

FIGURE 3. Scanning microprobe MS apparatus [19]

(a) Screening experimental set-up

(b) Gas delivery/removal/sample nozzle

(c) Photothermal deflection detector

FIGURE 4. High throughput screening of electrocatalysts by fluorescence indicators [12]

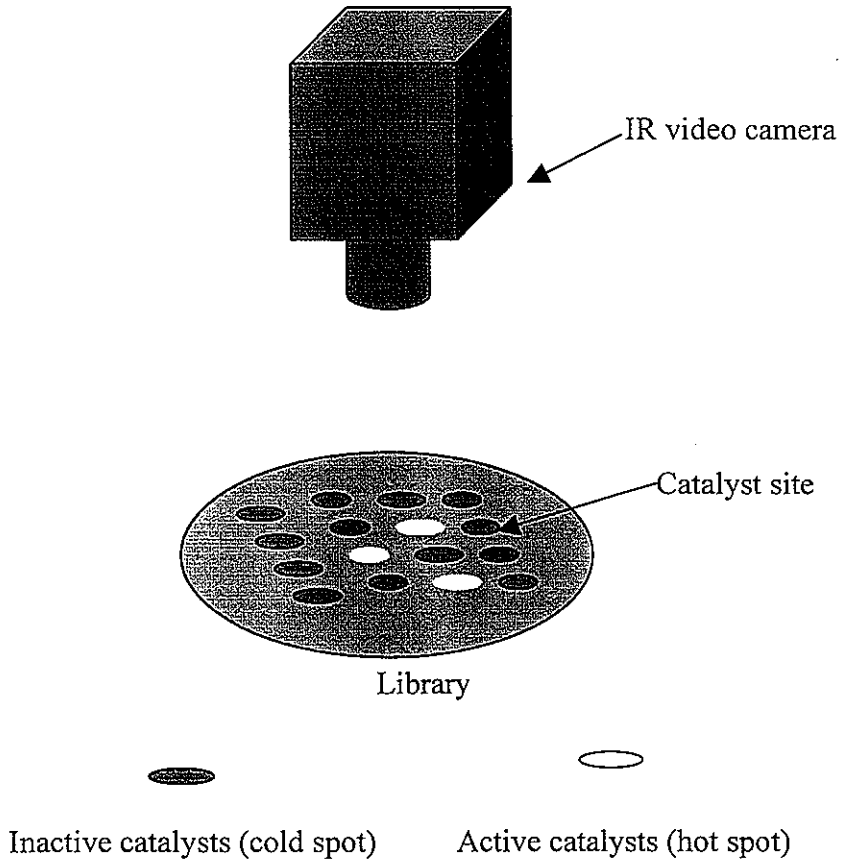
IR video camera
Catalyst site
Library
Inactive catalysts (cold spot)
Active catalysts (hot spot)

Figure 1

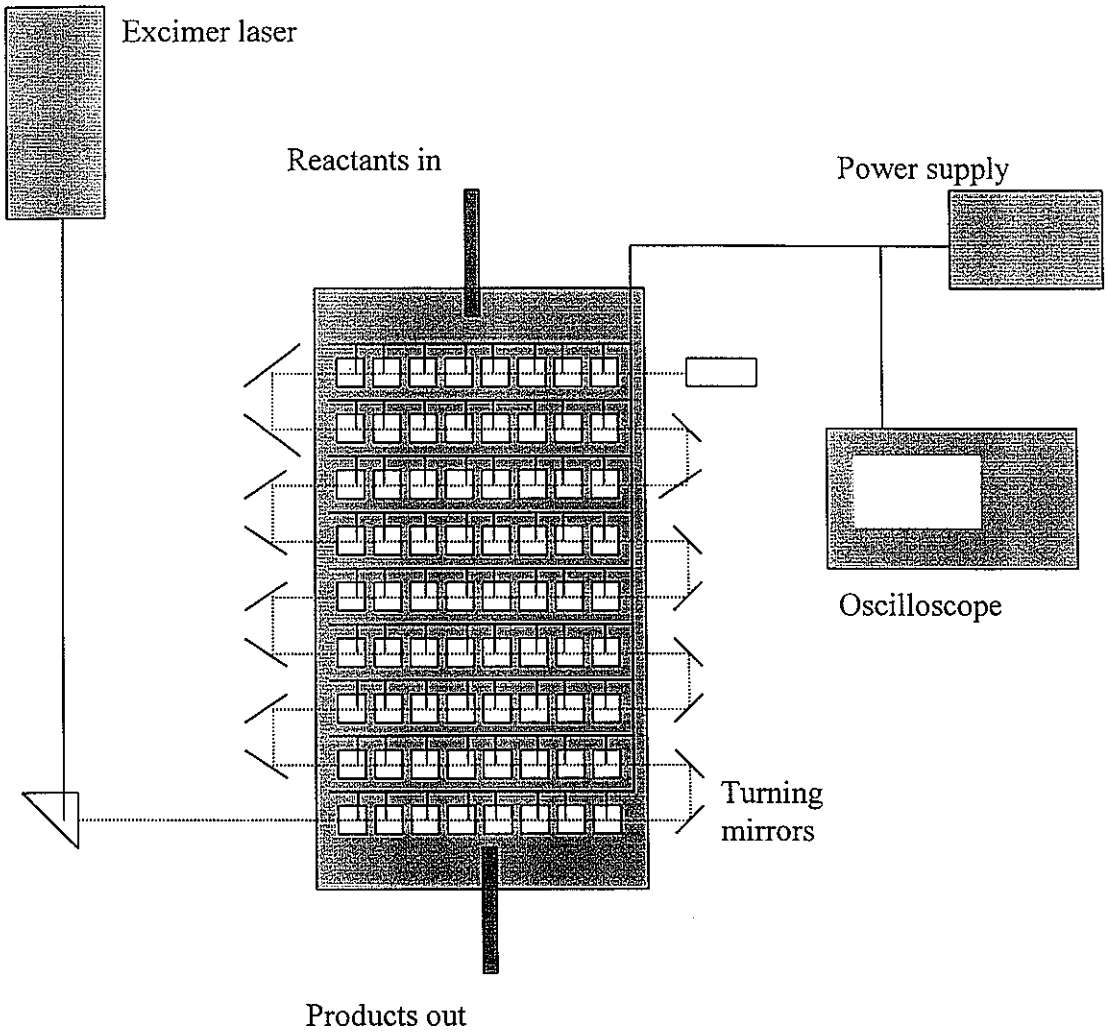
Excimer laser
Reactants in
Power supply
Oscilloscope
Turning
mirrors
Products out

Figure 2 (a)

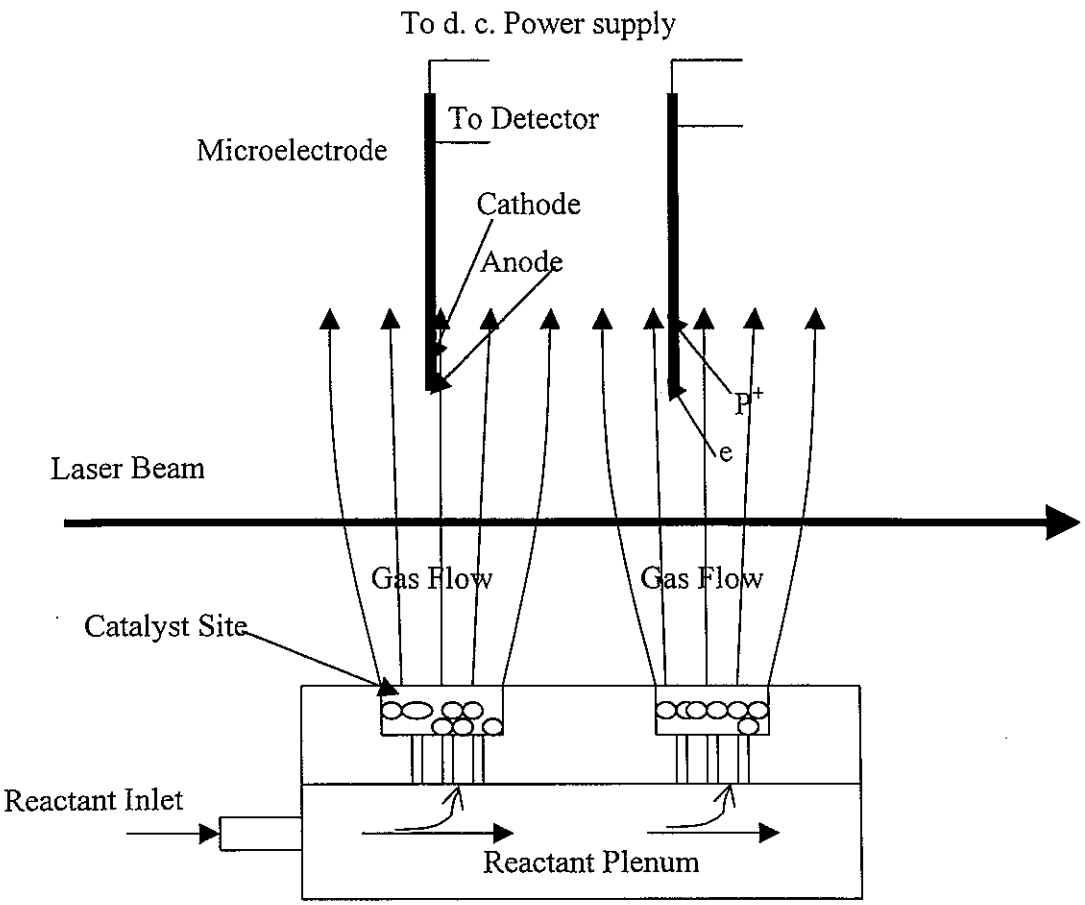
To d. c. Power supply
To Detector
Microelectrode
Cathode
Anode
P+
e
Laser Beam
Gas Flow
Gas Flow
Catalyst Site
Reactant Inlet
Reactant Plenum

Figure 2(b)

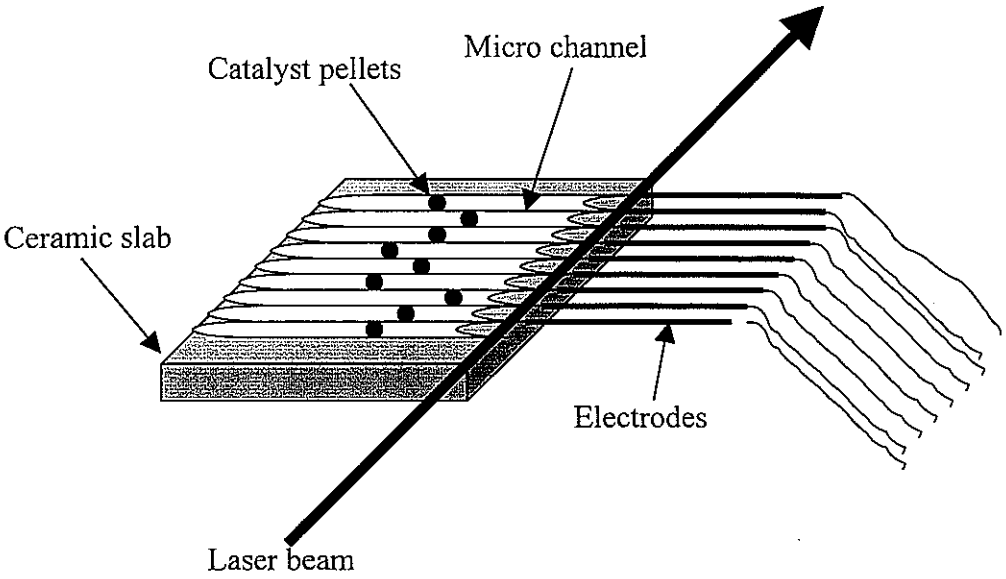
Catalyst pellets
Micro channel
Ceramic slab
Electrodes
Laser beam

Figure 2(c)

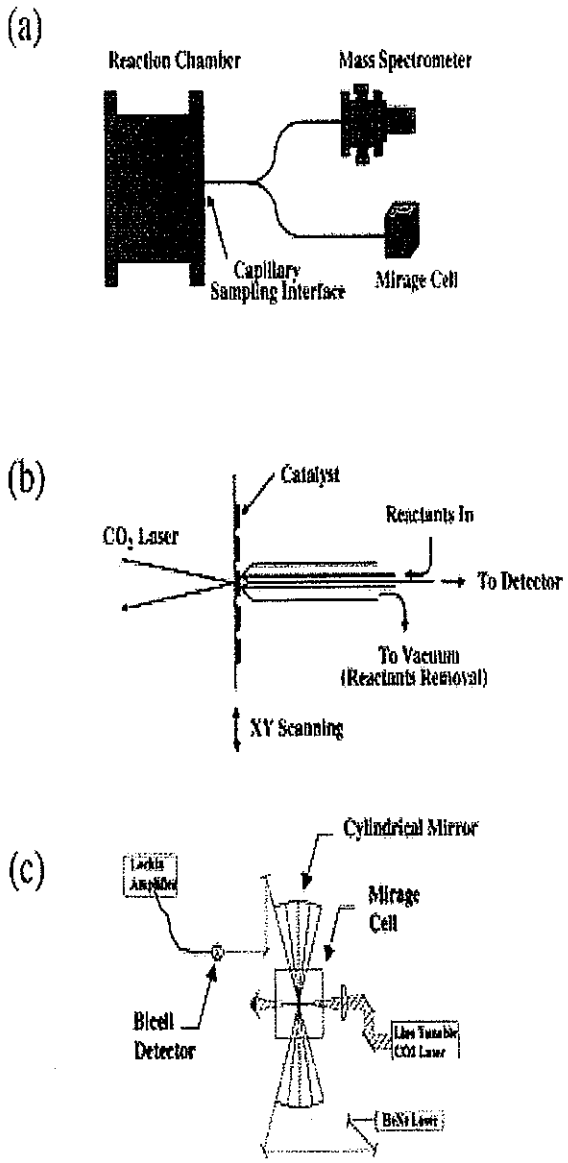
(a)
Reaction Chamber
Mass Spectrometer
Capillary
Sampling Interface
Mirage Cell
(b)
Catalyst
Reactants In
CO_2 Laser
To Detector
To Vacuum
(Reactants Removal)
XY Scanning
(c)
Cylindrical Mirror
Mirage
Cell
Bicell
Detector

Figure 3

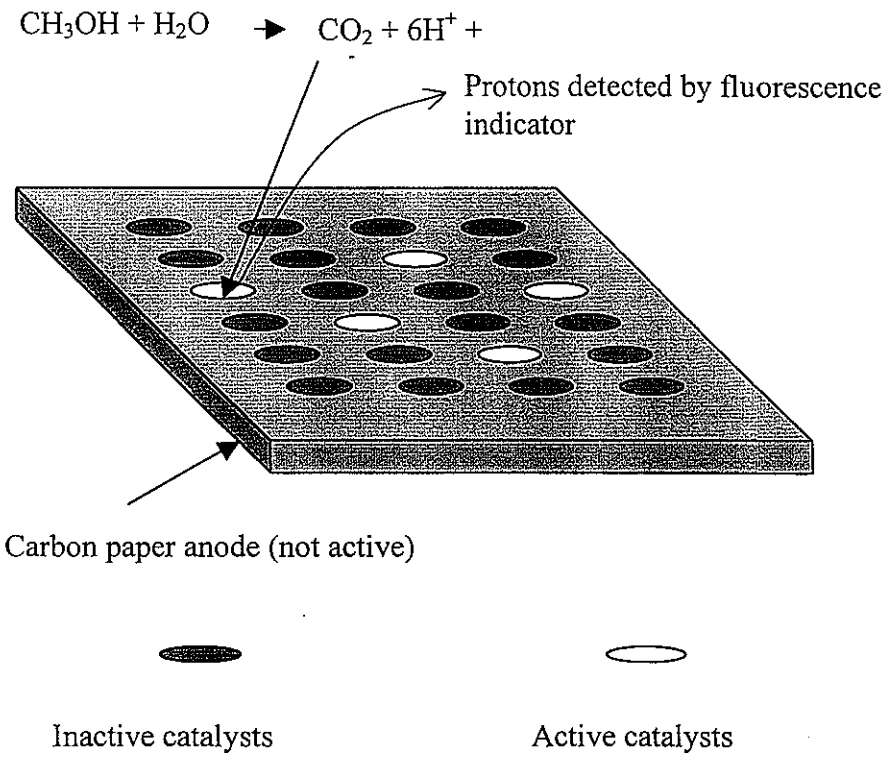
$CH_3OH + H_2O$
$CO_2 + 6H^+ +$
Protons detected by fluorescence indicator
Carbon paper anode (not active)
Inactive catalysts
Active catalysts

Figure 4

CHAPTER 2. HIGH-THROUGHPUT SCREENING OF HETEROGENEOUS CATALYSTS BY LASER-INDUCED FLUORESCENCE IMAGING

A paper published in Journal of American Chemistry Society

Hui Su and Edward S. Yeung

Catalytic gas processing is a multimillion-dollar concern in the chemical industry. A minor increase in the yield, a minor decrease in undesirable by-products, the creation of novel products, or an extension of the lifetime of the catalyst are all urgent issues. An efficient approach towards understanding these complex systems is through combinatorial assays. *In situ* screening of these arrays under continuous flow in a microreactor system will quickly reveal the best combination of catalyst and reaction conditions.

The power of combinatorial chemistry is apparent in medicinal chemistry research.[1] It is also developing rapidly into an attractive alternative to the traditional discovery process of heterogeneous catalysts. Combinatorial synthetic techniques based on gas-phase deposition and liquid dosing[2] allows us to prepare a large number of potential catalytic materials in a high-throughput fashion. Recently high-throughput screening methods by IR thermography,[3,4] laser-induced resonance-enhanced multiphoton ionization,[5] microprobe sampling mass spectrometry,[6] and fluorescence indicators[7,8] have been reported. In the present paper, we introduce laser-induced fluorescence imaging (LIFI) as an alternative for

high-throughput screening of heterogeneous catalysts *in situ* with micron-scale spatial resolution and millisecond temporal resolution. This scheme is based on the fact that the creation or destruction of chemical bonds alters the fluorescence properties of suitably designed molecules. By irradiating the region immediately above the catalytic surface (within 100 μm) with a laser, the fluorescence intensity of a selected product or reactant can be imaged by a charge-coupled device (CCD) camera to follow the catalytic activity as a function of time and space. Unlike thermography,[3,4] the fluorescence signal is specific and the response is linear. Interferences from variations in surface composition and the associated material emissivity are also absent. Secondary reactions do not contribute to the signal. Even thermoneutral reactions can be followed. Using this technique, dense arrays of catalyst formulations can be screened simultaneously to provide rapid access to the optimal combination of conditions.

We monitored the catalytic activity of vanadium pentoxide in the oxidation of naphthalene to naphthoquinone by oxygen, which is an important industrial process. With 488-nm excitation, naphthoquinone fluoresces while naphthalene and the other major product, phthalic anhydride, do not fluoresce. The reaction is carried out at 330-370 °C in a flow cell shown in Fig. 1. Fluorescence emission at 515-545 nm is collected by a cooled scientific CCD camera.

To evaluate the spatial resolution of LIFI, we used a 4× microscope objective to image a 2 mm × 2 mm area (Fig. 2) with 3 s exposure time. In this array, 400-μm diameter wells that are 400-μm deep are created on a stainless-steel plate with 400-μm spacing between them. No naphthoquinone fluorescence was detected above the V_2O_5 surface until

oxygen gas carrying 7% naphthalene is introduced into the reactor. Therefore, background signal can be recorded in the absence of the reactants and subtracted from each subsequent image. On comparing the optical image of the catalyst and the fluorescence image, a 20-μm shift in the flow direction can be observed. These experiments demonstrate that LIFI has good detection performance and the spatial and temporal resolution needed for high-throughput screening of heterogeneous catalysts. The sample packing density can therefore reach 250 × 250 subunits/cm^2 for 40-μm wells.

In a larger format, a 3 × 2 library that contained 6 identical V_2O_5 sample dots was prepared by pipetting 20-μg V_2O_5-cyclohexane slurry solution into small wells (2 mm wide and 0.5 mm deep with 2-mm spacing) on a stainless steel disc and dried in air. A camera lens instead of the microscope objective was used to image the 17 mm × 17 mm area. The variation in fluorescence among the wells is ± 1.1%. Detection of minor differences in catalytic activity is thus feasible.

The 3 × 2 library was then constructed with 6 sample dots with different amounts of V_2O_5 (10 μg, 20 μg, 30 μg, 40 μg, 50 μg and 60 μg), as shown in Fig. 3a. *In situ* fluorescence images of this library are shown in Fig. 3b. The relationship between catalytic activity (proportional to fluorescence intensity) and the amount of catalyst (Fig. 4) is not linear because catalytic activity is proportional to the available surface area, not the mass of the catalyst. At low amounts, there is residual contribution from the background of laser scatter and thermal emission. Then, the intensity increases because the surface area increases linearly with the amount present. As a thick layer is formed in the well, material buried at the bottom of the wells is shielded and no further increase in surface area is effected. This occurs

at 50 μg per well according to Fig. 4. When adapted to 40-μm wells, the amount of material need for screening will be 20 ng each.

We used LIFI to test a simple 3 × 2 binary library, as shown in Figure 3c. Samples 1 and 2 are pure V_2O_5, samples 3 and 4 are 1:1 TiO_2 and V_2O_5 mixtures, and samples 5 and 6 are pure TiO_2. Fig. 3c indicates that TiO_2 does not catalyze the oxidation of naphthalene to naphthoquinone, and also neither promotes nor suppresses the catalytic activity of V_2O_5 in this reaction.

We studied the difference between LIFI and IR thermography in the system shown in Fig. 2. At 330 °C, only fluorescence can be observed by this CCD camera. At and above 350 °C, however, elevated intensities can be detected in the wells above the background level (stainless steel portions of the plate) even in the absence of laser irradiation. This is near-IR emission from the catalytic material as a result of the exothermicity of the reaction, i.e., IR thermography. The camera is sensitive to radiation down to around 1000 nm. This is sufficient to record the short-wavelength tail of the blackbody radiation from the source. Because of the low dark count and low read noise of the camera, flat fielding (subtraction of the image from background levels) reveals a thermal image. The blackbody behavior is confirmed by placing short-pass filters in front of the camera at successively longer and longer wavelengths between 800 and 1000 nm.

For studies conducted between 330-370 °C, the lower temperature favors S/N for LIFI while the higher temperature favors S/N for thermography. The spatial resolution of thermography is limited only by the pixel resolution of the imaging system while that of LIFI is further limited by the 20-μm flow distortion. In this set-up, both sets of information can be obtained by chopping the laser irradiation or by rotating filters between the visible and near-

IR. We note that CCD thermography is only useful at these high temperatures when black-body emission begins to reach the responsive region of the device. When it does, the combination of non-specific temperature increase and species-specific concentration maps offers unique insights into the catalytic process. Finally, the catalytic system here happens to involve fluorescent species. However, it should be possible to design model reactants for just about any catalytic reaction so that either the reactant or the product fluoresces on the breaking or making of the bond of interest.

Acknowledgement

We thank Dr. Glen Schrader for help in designing the reactor and for providing the catalysts. The Ames Laboratory is operated for the U.S. Department of Energy by Iowa State University under Contract No. W-7405-Eng-82. This work was supported by the Director of Science, Office of Basic Energy Sciences, Division of Chemical Sciences.

References

1. Whiting, A. Chemistry in Britain Mar. 1999, 31-34.
2. Sun, X. D.; Wang, K. A.; Yoo, Y.; Wallace-Freedman, W. G.; Gao, C.; Schultz, P.G. Adv. Mater. 1997, 9, 1046-1049.
3. Moates, F. C.; Somani, M.; Annamalai, J.; Richardson, J. T.; Luss, D.; Wilson, R. C. nd. Eng. Chem. Res. 1996, 35, 4801-4803.

4. Taylor, S.J.; Morken, J. P. Science 1998, 280, 267-270.

5. Senkan, S. M. Nature 1998, 394, 350-353.

6. Cong, P.; Doolen, R. D.; Fan, Q.; Giaquinta, D. M.; Guan, S.; McFarland, E. W.; Poojary, D. M.; Self, K.; Turner, H. W.; Weinberg, W. H. Angew. Chem. Int. Ed 1999, 38, 484-488.

7. Reddington, E.; Sapienza, A.; Gurau, B.; Viswanathan, R.; Sarangapani, S.; Smotkin, E. S.; Mallouk, T. E. Science 1998, 280, 1735-1737.

8. Miller, S. J.; Copeland, G. T. J. Am. Chem. Soc. 1999, 121, 4306-4307.

FIGURE CAPTIONS

Figure 1. Experimental arrangement for *in situ* spatial and temporal measurements of catalytic activity. The laser beam (300 mW) is focused into a sheet parallel to the surface to excite the product molecules such that the recorded fluorescence intensity reflects the local reaction rate.

Figure 2. Fluorescence imaging of reaction products on top of an array of V_2O_5 wells that are each 400-μm diameter, 400-μm deep and with 400-μm spacing in between.

Figure 3. Catalytic screening by fluorescence imaging. (a) Optical image of six 2-mm diameter wells with 2-mm spacing in between each containing different catalysts. (b) Fluorescence image of naphthoquinone produced above each well of vanadium pentoxide for 1 – 60 μg, 2 – 50 μg, 3 – 40 μg, 4 – 30 μg, 5 – 10 μg, and 6 – 20 μg. (c) Fluorescence image of naphthoquinone produced above each well for 50 μg of 1 and 2 – pure vanadium pentoxide, 3 and 4 – 1:1 vanadium and titanium oxides, and 5 and 6 – pure titanium oxide.

Figure 4. Fluorescence intensity (activity) as a function of the amount of catalyst in each well in Fig. 3b.

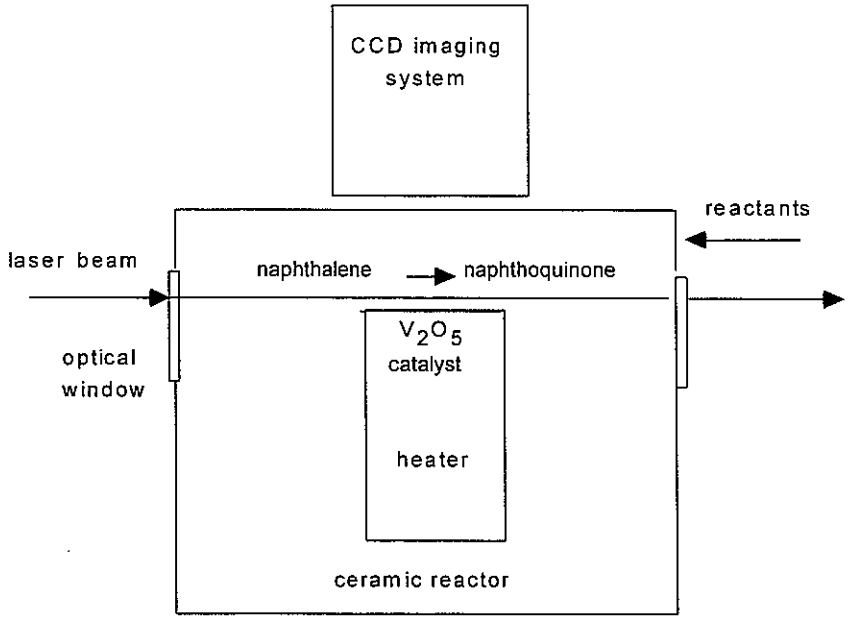
CCD imaging system
reactants
laser beam
naphthalene
naphthoquinone
optical window
V_2O_5 catalyst
heater
ceramic reactor

Figure 1

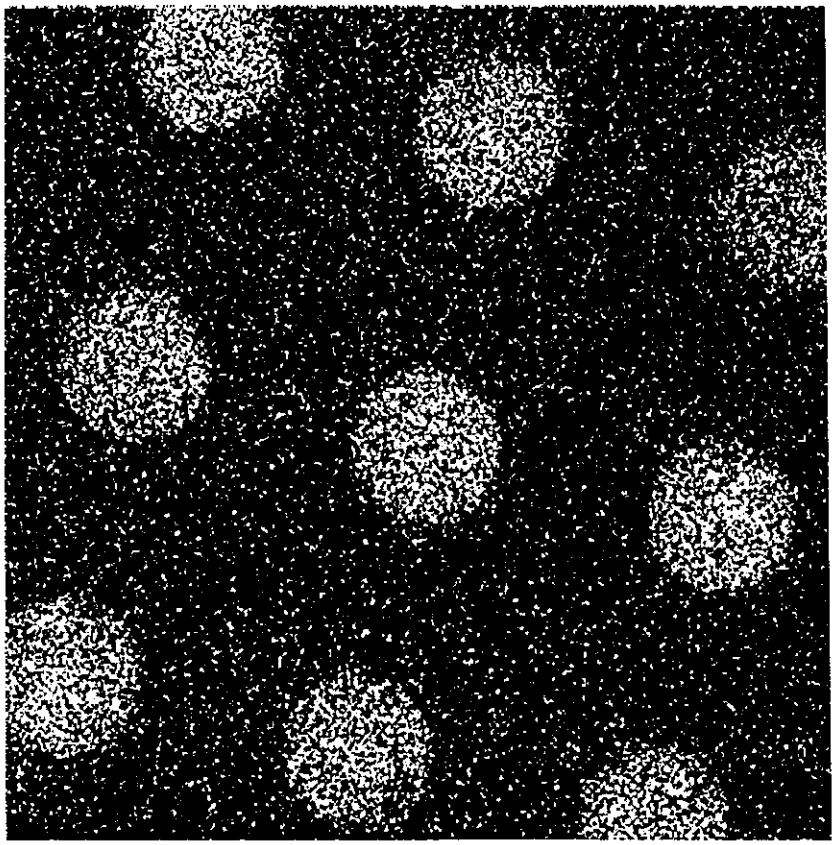

Figure 2

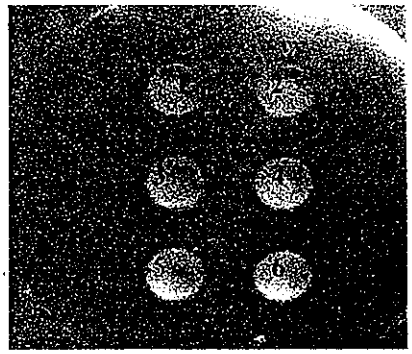

(a)

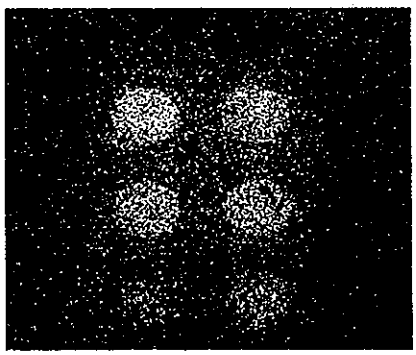

(b)

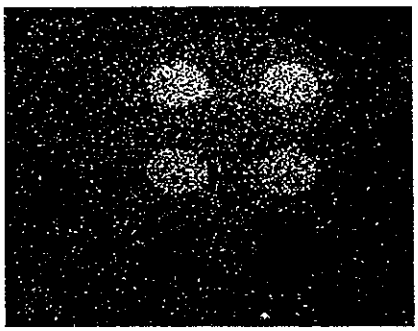

(c)

Figure 3

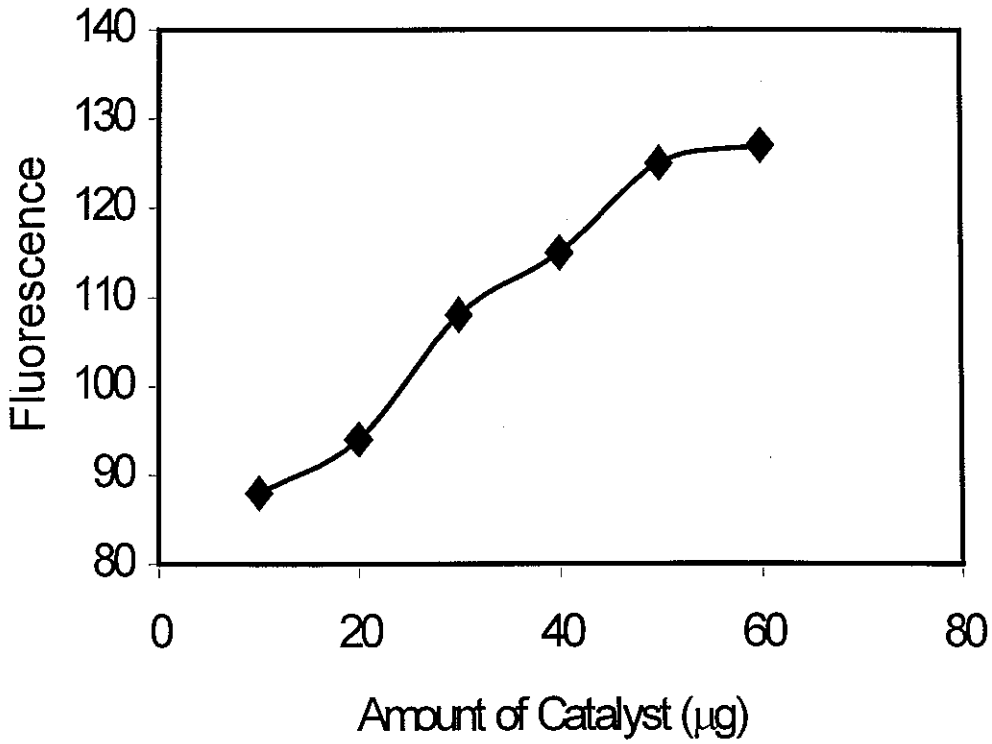
140
130
120
110
100
90
80
Fluorescence
0
20
40
60
80
Amount of Catalyst (µg)

Figure 4

CHAPTER 3. COMBINATORIAL SCREENING OF HETEROGENEOUS CATALYSTS IN SELECTIVE OXIDATION OF NAPHTHALENE BY LASER-INDUCED FLUORESCENCE IMAGING

A paper prepared for submission to Analytical Chemistry

Hui Su and Edward S. Yeung

Abstract

Heterogeneous catalysis is one of the most important processes in petroleum and chemical industries and would be improved by improving the performance of heterogeneous catalysts. To be able to screen catalysts, a high throughput rate will dramatically shorten the catalyst discovery process. Here, we use Laser-induced fluorescence imaging (LIFI) as a high-throughput screening (HTS) technique in combinatorial discovery active catalysts for naphthalene oxidation. Binary catalysts of V-Mo-O, V-Sn-O, V-Ti-O and V-W-O in a 15-membered library were screened under the fluorescence and IR detectiom modes. The addition of MoO_3, WO_3, SnO_2 and TiO_2 in V_2O_5 do not improve the catalytic activity of V_2O_5 in catalyzing naphthalene to naphthoquinone, but increase of overall activity was observed in certain binary samples. The screening result by LIFI for 15-membered library of ternary catalysts of V-Sn-Mo-O revealed that the combination of V (45%)-Sn (45%)-Mo (10%) gave 70% higher catalytic activity than pure V_2O_5 in catalyzing naphthalene to naphthoquinone. Temperature and sample preparation effects on catalytic activity and

selectivity of catalyst are studied by LIFI in a high-throughput way. Laser ablation ICP -MS is demonstrated to perform composition analysis for individual catalysts in a combinatorial library without damaging the library.

Introduction

Nowadays combinatorial chemistry has fundamentally changed the concept and process of discovery, and high-throughput screening (HTS) assures the power of combinatorial chemistry. In the area of heterogeneous catalyst development, various promising techniques based on thin film deposition and liquid dosing[1] have been developed to provide a large number of catalytic materials in a high-throughput fashion, and HTS of heterogeneous catalysts seem to be more challenging compared with their synthesis. Recently IR thermography,[2-4] laser-induced resonance-enhanced multiphoton ionization,[5] microprobe sampling mass spectrometry,[6,7] and fluorescence indicators [8,9] have been used, but they all have their inherited limitations. IR thermography is capable of screening the overall activities for hundreds and thousands of catalysts either in gas-solid or liquid-solid exothermic reaction by measuring the temperature changes of the catalysts. Since IR thermography is not chemically specific, in certain circumstance the information provided by it might be misinterpreted. Provided that two (or more) exothermic conversions, A and B, are involved in one catalytic system, conversion A has much higher enthalpy than B, catalyst (H) with high selectivity towards A will have larger temperature change than catalyst (L) that is favorable to B at the same conversion level. In this case, a very selective catalyst (L) probably will be discarded because of its low signal in IR thermography. Multiphoton ionization and fluorescence indicator techniques have limited applications because of their

restricted fundamental requirements. So far, microprobe sampling MS is the most successful HTS method for heterogeneous catalysts, but it is basically a robust scanning technique, not a real combinatorial screening methodology, time and cost are still the issue here.

Recently, we have proposed laser-induced fluorescence imaging (LIFI) as an alternative for HTS of heterogeneous catalysts. [10] LIFI has good detection performance and the spatial and temporal resolution needed for HTS of heterogeneous catalysts. The application of LIFI as a HTS technique for heterogeneous catalysts is also very promising because creation or destruction of chemical bonds alters the fluorescence properties of molecules, which is the case in most of the heterogeneous catalytic reactions. As a combination of selective fluorescence detection and 2-dimentional imaging technique, LIFI is capable of screening up to 250×250 subunits/cm^2 (40-μm diameter / subunit) simultaneously. [10] Furthermore, since the CCD camera is sensitive to radiation in the near-infrared region, high-throughput screening based on IR thermography detection can be performed by monitoring the temperature changes of catalysts on the same instrumentation with the right combination of optics. Unification of LIFI and IR thermography on a single instrument enables us to access unique information of the catalytic system in a simple and efficient way.

Selective oxidation is a very important industry process that is used to manufacture a variety of chemicals. Vanadium pentoxide catalysts are used as the selective catalysts for oxidation of aromatic in industry. Various promoters are frequently added to vanadium pentoxide to improve the selectivity and activity to desired products. The surface active sites of V_2O_5 under the promoting effect of WO_3, [11] MoO_3 [12] and SnO_2[13] have been investigated, and the surface concentration of redox sites was found increased significantly at the present

of these oxides. The activity and selectivity of the promoted vanadium pentoxide catalysts in selective oxidation of benzene to maleic anhydride (MA) have been tested by gas chromatography analysis.[14] The addition of less electronegative elements, MoO_3 and WO_3, were found to able to increase the selectivity to MA by lower the activity of redox sites to the optimum leverl in the selective oxidation of benzene; on the other hand, the addition of more electronegative element, SnO_2, resulted in decrease in the selectivity to MA.

In this work, we will use LIFI and IR theromography to screen the activity and selectivity of binary vanadium-based catalysts of V-Mo (VI)-O, V-W (VI)-O, V-Sn (IV)-O and V-Ti (IV)-O for selective catalytic oxidation of naphthalene to naphthoquinone, which is the competing product of phthalic anhydride (PhA). Based on the screening results of binary libraries, we prepared and screened ternary 15-membered libraries of V-Sn-Mo and V-Sn-W. Composition of components and sample preparation methods are two variables in constructing the libraries. The temperature effect on the catalytic performance on catalysts is also studied by monitoring the catalytic reaction at different reaction temperatures. We also demonstrated in this paper that the composition analysis of individual catalysts on library could be accomplished by LA-ICP-MS without damaging the library itself.

Experimental Section

Laser-induced Fluorescence Imaging System

Schematic diagram of the laser-induced fluorescence imaging system is shown in Figure 1. An Ar+ laser (Coherent Laser Group, Santa Clara, CA) is used to irradiate the region right above the catalyst in a catalytic reaction, the fluorescence intensity of a selected product or reactant can be imaged by a frame transfer CCD camera (Roper scientific,

Trenton, NJ). Laser beam is focused into a laser sheet by a cylindrical lens combination. In present work, a 488-nm wavelength is chosen to excite naphthoquinone in the oxidation reaction of Naphthalene catalyzed by vanadium-based catalysts, and a 50-mm lens (Nikon, Japan) collects the fluorescence emission of naphthoquinone from 515nm to 545nm. All the images are stored and processed in computer by Winview (Roper Scientic, Trenton, NJ).

Infrared Imaging

This LIFI detection system can be switched to infrared imaging detection mode simply by removing a hot mirror that blocks the infrared emission (>700nm) in LIFI, laser excitation is not needed in IR detection.

Excitation of Laser Sheet

In order to excite the product or reactant above the catalyst homogeneously, a laser sheet instead of a laser beam is desired (figure2 (a)). A laser beam can be focused into a laser sheet by a 2-m cylindrical lens, which has a 12-mm of depth of focus (x) and 78-μm waist radius at the focal plane (y). Then a homogeneous irradiation in X and Y direction for the product or reactant can be achieved by placing the catalyst library right underneath the laser focal "band". The nature of Gaussian distribution remains in the laser sheet, which contribute the inhomogeneous laser power distribution in the Z direction. One way to achieve relatively homogeneous laser power distribution in Z direction is to pass laser beam through a line generator lens before it focuses on the cylindrical lens. Since only middle platform of the laser beam (figure2 (b)) can be used as homogeneous irradiation after passing through line generator lens, a high power laser is needed. The other way is to calibrate the fluorescence

signal by laser scattering background. In this paper, all the image data were generated in Gaussian laser sheet and calibrated by scattering background.

Data Calibration

Two calibrations are needed in LIFI detection. One is the laser scattering background, which can be corrected by deduction of library image before reaction from fluorescence images taken during the reaction; another is to calibrate the laser power. Gaussian distribution of energy in laser sheet (or beam) can generate false screening information because the fluorescence signal is proportional not only to the activity of catalyst but also to the laser power. The intensity of Rayleigh scattering of laser beam is proportional to laser energy, which makes a perfect calibration of laser energy for the fluorescence emission. The calibration can be accomplished by diving fluorescence image by scattering background image, the intensity of corrected image is only proportional to the activity of the catalyst.

Flow Cell Reactor System

The reactor is a cylindrical stainless steel vessel with an inner diameter of 4cm and a depth of 3cm (shown in figure 3). The cylindrical sample holder with an outer diameter of 1.3cm and a height of 2cm is in the middle of the reactor and a cartridge heater (Omega, Stamford, Connecticut) is buried in the sample holder cylinder. A thermocouple (Omega, Stamford, Connecticut) is buried underneath the top of the sample holder, and a temperature control unit (Omega, Stamford, Connecticut) is used to control the reaction temperature. Two optical windows are placed on the wall of the reactor to pass the laser beam immediately above the top of the sample holder. Reactant mixture gas is introduced into the reactor from

the entrance port, and pumped out from the exit port located on the other side of the reactor. A stainless steel oven with heating device and temperature control unit (Omega, Stamford, Connecticut) is used as reactant cell to provide reactant feed with desired concentration. In this work, 7%of naphthalene is carried into reactor by O_2 by heating the naphthalene at 135°C.

Catalyst Preparation

Binary catalysts of V_2O_5-MoO_3, V_2O_5-WO_3, V_2O_5-SnO_2, V_2O_5-TiO_2 with atomic ratio of 9, 2.33, 1, 0.43 and 0.11 are prepared in two ways. Method (A) Mix the oxides of two elements. (B) Mix the oxalic acid solution of NH_4VO_3 with $(NH_4)_2MoO_4$, $(NH_4)_2WO_4$, Sn $(OH)_2$ and TiO_2 respectively followed by evaporation drying overnight and subsequent calcination in flow of O_2 at 773K for 3h.

Ternary catalysts of V-Sn-W and V- Sn- Mo were prepared by method B, and the composition of these catalysts are mixture of 5%, 10% and 15% of Mo or W with 9, 2.33, 1, 0.43 and 0.11 (atomic ratio) of V-Sn.

Catalyst Library

A catalyst library is prepared by pipetting 1-μl of vanadium catalyst-cyclohexane slurry solution into small wells (1mm wide and 0.5mm deep with 1-mm spacing) on a stainless steel disk with a diameter of 1.3 cm) shown as figure 4. 8 libraries were tested in this paper, libraries 1-4 are made of binary samples: A1-A5 samples are prepared by method (A), B1-B5 by method (B) and C1-C3 are pure V_2O_5.

Library 1: V (90%) / Sn (10%) (A1, B1), V (70%) / Sn (30%) (A2, B2), V (50%) / Sn (50%) (A3, B3), V (30%) / Sn (70%) (A4, B4), V (10%) / Sn (90%) (A5, B5), V_2O_5 (100%) (C1-C3), SnO_2 (100%) (C4-C5).

Library2 (V-Ti), library3 (V-Mo) and library (V-W) use the same arrange as that in library1.

Library5-8 are ternary samples.

Library5: A1: Mo (5%)/ V (85.5%) / Sn (9.5%); A2: Mo (5%)/ V (66.5%) / Sn (28.5%); A3: Mo (5%)/ V (47.5%) / Sn (47.5%); A4: Mo (5%)/ V (28.5%) / Sn (66.5%); A5: Mo (5%)/ V (9.5%) / Sn (85.5%); B1: Mo (10%)/ V (81%) / Sn (9%); B2: Mo (10%)/ V (63%) / Sn (27%); B3: Mo (10%)/ V (45%) / Sn (45%); B4: Mo (10%)/ V (27%) / Sn (63%); B5: Mo (10%)/ V (9%) / Sn (81%); C1: Mo (15%)/ V (76.5%) / Sn (8.5%); C2: Mo (15%)/ V (59.5%) / Sn (25.5%); C3: Mo (15%)/ V (42.5%) / Sn (42.5%); C4: Mo (15%)/ V (25.5%) / Sn (59.5%); C5: Mo (15%)/ V(8.5%) / Sn (76.5%).

Library6: A1-A2: V_2O_5; B1: V (90 / Sn (10%); B2: V (70%) / Sn (30%); B3: V (50%) / Sn (50%); B4: V (30%) / Sn (70%); B5: V (10%) / Sn (90%); C1: Mo (10%)/ V (81%) / Sn (9%); C2: Mo (10%)/ V (63%) / Sn (27%); C3: Mo (10%)/ V (45%) / Sn (45%); C4: Mo (10%)/ V (27%) / Sn (63%); C5: Mo (10%)/ V (9%) / Sn (81%).

Library7 has the same arrangement as library5 substituting Mo with W as well as library 6 and library8.

Laser-ablation ICP-MS

The experiments were performed with a Finngann MAT (San Jose, CA) ICP -MS and 266-nm laser ablation system (CETAC, IA). The 266-nm Nd:YAG laser was operated at

10Hz with typical pulse energy of 10mJ. Single spot sampling was used and 3 samples were taken for each catalyst. ICP-MS was operated at medium resolution range with Rf power of 1200W.

Reactants

99% Naphthalene (Sigma, MO); 99.99%V_2O_5, 99.99%WO_3, 99.99% MoO_3, 99.9% SnO_2, 99.9% $(NH_4)_2MoO_4$, 99.9%$(NH_4)_2WO_4$ (Aldrich Chem., WI); 99.9% cyclohexane (Fisher Scientific, NJ).

Results and Discussion

Selective Oxidation of Naphthalene

The selective oxidation of naphthalene (NA) can be catalyzed by V_2O_5 at elevated temperature, and there are two major products in this reaction:

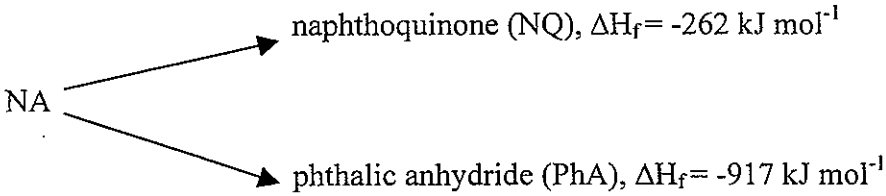

Here we screen the selective catalytic activity (relative) of catalysts by monitoring the fluorescence intensity of NQ produced in the reaction by LIFI, and overall catalytic activity (relative) by monitoring the temperature change of the catalysts by IR imaging since both major reactions are exothermic.

Combinatorial Screening of Binary Heterogeneous Catalysts

In search of active catalysts, usually we want to start with binary samples and look for possible trends in term of compositions and sample making, and then we go from there to

more complex systems, ternary, quaternary, etc. Since the discovery of catalysts still bases on experimental results, the high-throughput capability of LIFI provides the convenience of fast pre-selection of useful components from a large diversity.

Vanadium Pentoxide is an effective catalyst for catalytic oxidation of naphthalene (NA) to naphthoquinone (NQ) and phathalic anhydride (PA). Addition of foreign oxides into V_2O_5 might change its catalytic activity and selectivity by modifying its surface active sites. Sample preparation also has an important effect on the performance of catalysts. The catalytic reactions carried on libraries 1-4, which consist of binary catalysts prepared in two different ways, were monitored in both fluorescence and infrared detection mode. Since only the fluorescence emission of NQ was collected in LIFI, the fluorescence intensity of individual catalyst spot represents its relative catalytic activity for NQ. Intensity of infrared emission of individual catalyst is proportional to the total activity for all the exothermic reactions involved.

In library1, both fluorescence (figure5a) and IR images (figure5b) detection show pure V_2O_5 is active in this catalytic reaction and pure SnO_2 is inactive. Addition of SnO_2 decreases the activity of V_2O_5 for NQ (figure5c), stronger depression of activity (NQ) is observed in catalysts prepared by method (A) than catalysts prepared by method (B). The total activity of A catalysts (Figure5c) is enhanced by SnO_2 (10%, 30% 50%) and depressed activity of As comes with further increase of SnO_2. On the other hand, total activity of B catalysts increases with the addition of SnO_2; a maximum increase of 67% was obtained in a B catalyst of V_2O_5 (10%)-SnO_2 (90%) (Figure5c). The only explanation of the decrease in activity for NQ and increase in total activity for one catalyst is that the other product in this catalytic reaction, PA, is favored in the presence of certain amount of SnO_2. In reference 14,

the reaction rate of maleic anhydride (MA) in selective oxidation of benzene reached maximum at the presence of 40% or 80% of SnO_2 in V_2O_5 prepared in two different ways respectively, which is not very far from what we got from out screening results, 50% and 90%. Although different sample preparation methods are involved in these two experiments, we still can conclude that the addition of SnO_2 can increase the concentration of surface active sites and the amount of SnO_2 will affect the activity of these surface redox sites provided that the concentration of surface active sites decides the reaction activity and the activity of surface sites determine the selectivity of a catalyst.

Library 2 consists of 8 binary samples of V_2O_5-TiO_2 with different ratios and prepared in different ways. From the fluorescence detection (figure6a), infrared detection (figure6b) and their comparison (figure6c), TiO_2 has negative effect on the total activity and NQ activity of V_2O_5 in selective oxidation of benzene for both A and B catalysts, which might be caused by dilution of active sites of V or surface modification of the catalysts by TiO_2. For As, similar decreases in activity for NQ and total activity are shown in figure 6c. Dilution effect should be dominant because the modification of active sites should change the selectivity of the catalyst, and the changes in total activity and activity for NQ (slope) should be different (different reaction heat for two products). For B catalysts, changes in total activity of sample B1 to B3 are larger than changes in NQ activity, we can predict that not only dilution effect of inactive Ti oxide but also surface modification by Ti take place for B catalysts. The depression of overall catalytic activity of vanadium pentoxide by the addition of TiO_2 suggests that the concentration of surface active sites on vanadium pentoxide can't be increased at the presence of TiO_2.

The V-Mo binary catalyst is a very interesting catalytic system. Both V_2O_5 and MoO_3 are catalytically active according to figure 7a and 7b. As in figure7c, the addition of MoO_3 up to 50% decreases the catalytic activity of vanadium in selective oxidation of NA to NQ, and further increase of Mo results in increase in the activity. This result agrees well with the reported results. [14] However, the screening result from IR imaging doesn't cooperate this conclusion (figure7b, 7c). The addition of MoO_3 was reported to increase the overall activity as well as the activity of selective oxidation of benzene to MA. The result shown in figure 7b goes the other way. From our experiment results, the addition of Mo (VI) decreased the selective activity of V_2O_5 in oxidation of NA to PhA. One explanation for this result is the difference of activity of surface active sites in production of MA and PhA. Sample A2 and B2 have the sampe composition and similar activity for NQ, but A2 shows higher overall activity, which means the surface active sites of catalysts made in method B are less favorable to the formation of PhA. Catalyst B5 has a slightly higher catalytic activity than pure vanadium pentoxide in selective oxidation of NA to NQ while the IR detection shows that it is much less active than pure vanadium, which shows us that IR thermography screening is not highly accurate in one way or the other.

Different catalytic behaviors between V-W catalysts prepared by different methods are demonstrated in figure 8(a), (b) and (c), but none of these combinations gives better performance than pure V_2O_5 either in overall activity or activity for NQ in selective oxidation of NA. Again, we are seeing difference in promotion effect of W in selective oxidation of benzene and naphthalene compared to the results in reference 14.

Screening of Ternary Heterogeneous Catalysts

Based on above experiment results, Mo, Sn and W seem to be able to modify the active sites of vanadium catalyst in their own ways especially prepared by method B based on what we have seen above. Then we prepared library 5, which consists of V-Sn-Mo-O and V-Sn-W catalysts in various ratios respectively. The screening results of selective activity by LIFI as well as the overall screening results by IR imaging for these catalysts are shown in figure9 (a)-(b). In library 5, the combinations of V (63%)-Sn (27%)-Mo (10%) and V (45%)-Sn (45%)-Mo (10%) are the most active catalysts in selective oxidation of NA to NQ. Compare the selective activities of these two combinations with pure V_2O_5 in library 6 (figure c and d), V (45%)-Sn (45%)-Mo (10%) demonstrate a 70% increase. The interesting result here is the overall activity of this promoted combination shown in figure 9d; the overall activity of V (45%)-Sn (45%)-Mo (10%) is depressed dramatically compared to pure V_2O_5. The combination we found in our screening results, V (45%)-Sn (45%)-Mo (10%), are much more active and selective in selective oxidation of NA to NQ than the conventional catalyst used in industry, V_2O_5.

Libraries 7 and 8 consist of V-Sn-W ternary catalysts prepared by method B. Catalysts with 10% W in library 7 seem to be more active in conversion of NA to NQ, but not as active as V_2O_5. Addition of 10% W into V (30%)-Sn (70%) increases its activity for NQ, and depresses its total activity; therefore we can predict that the conversion to PA is less favorable at the presence of W in V-Sn catalysts.

Temperature Dependency of Catalytic Activity

It is important to locate a suitable temperature range for a heterogeneous catalyst since its activity and selectivity is temperature dependent. Ternary library5 was screened by LIFI at temperature 603k, 613K, 613K, 623K, and 633K, the fluorescence images of the catalysts (figure10) show that different materials demonstrate different sensitivities to temperature changes. In library5, B samples with 10% Mo are among the most active catalysts, therefore they were chosen to be further screened in library6 with pure vanadium pentoxide and catalysts that have the same V-Sn composition but no Mo at different reaction temperatures. Since we have known that binary V-Sn materials are less active than pure vanadium pentoxide in conversion of NA to NQ, only the screening results of ternary V-Sn-Mo are compared with vanadium oxide (Mo=0%, Sn=0%) in figure11. We can see from the comparison that addition of 10% Mo boosts the activity of V/Sn (7/3), V/Sn (5/5) and V/Sn (3/7), and the activity enhancement varies as the temperature changes. At lower temperatures (up to 633K), V (63%)-Sn (27%)-Mo (10%) is more active than V (45%)-Sn (45%)-Mo (10%); but at temperatures about 633K, V (45%)-Sn (45%)-Mo (10%) is more active than V (63%)-Sn (27%)-Mo. All the catalysts in this library reach their activity high around 633K except V (45%)-Sn (45%)-Mo (10%) in this temperature range.

Composition Analysis by LA-ICP-MS

LIFI can access the catalytic performance of individual catalyst in a large format library, which generates our concern for composition analysis for the catalysts in the library prepared by thin film or evaporation technologies. Since more than one characterization probably will be needed for certain interesting catalytic materials (after screening), a desired

characterization method should be able to access solid materials directly in the library and cause as little as possible damage to the library itself. In many ways, Laser-ablation ICP MS seems to be a good choice.

In library3, Catalysts were analyzed by LA-ICP-MS. Single-spot sampling was used, and 3 spots were sampled for each catalyst (figure12). Since different elements have different absorption coefficients for 266-nm laser and different sensitivities in MS, a calibration is needed for composition analysis. In theory, Intensities of MS signals of individual compound are proportional linearly to their concentrations; therefore the intensity ratios of two elements should be proportional to the concentration ratios of these two elements. According to the 3-point calibration curve shown as figure13, 74% and 33% of Mo is found in sample B2 and B4. The real percentages of Mo in these two catalysts are 70% and 30, and the relative errors of the analysis are less than 6%.

Conclusion

In this work, we have demonstrated the application of Laser-induced fluorescence Imaging (LIFI) as a combinatorial screening technique for heterogeneous catalysts. We also demonstrate here that fluorescence imaging and infrared thermography can be unified in one instrument and specific information of more than one conversion can be obtained by comparing their side by side screening results. Laser-induced fluorescence Imaging was used in combinatorial screening of 8 libraries in catalytic oxidation of naphthalene.

There are several conclusions we can make based on our screening experiments: (1) The addition of Mo, W in vanadium pentoxide modifies the surface active sites, but does not increase the activity and selectivity of selective oxidation of naphthalene to phthalic

anhydride while it does increase the activity and selectivity of selective oxidation of benzene to maliec anhydride as reported in literatures. SnO_2 behaves similar to what it was reported. (2) Ternary samples of V (63%)-Sn (27%)-Mo (10%) and V (45%)-Sn (45%)-Mo (10%) were found having up to 70% higher activities than pure vanadium pentoxide as well as improved selectivity in conversing naphthalene to naphthoquinone. (3) Combinatorial studies of temperature dependency of catalytic activity have been accomplished by LIFI. (4) We demonstrate in this paper that LA-ICP-MS is capable of providing composition analysis for catalysts in the library with enough accuracy, which has no needs of sample preparation and causes no damages to the library.

By LIFI, we can screen solid heterogeneous catalysts at a speed of 15s per library. The screening throughput is hundreds times faster than conventional approach (calculation based on 15-membered library), it also top the other selective high-throughput screening techniques.

Acknowledgement

We thank Dr. Robert S. Houk and Yongjin Hou for assistance in LA-ICP-MS analysis of solid catalysts. The Ames Laboratory is operated for the U.S. Department of Energy by Iowa State University under Contract No. W-7405-Eng-82. This work was supported by the Director of Science, Office of Basic Energy Sciences, Division of Chemical Sciences.

References

1. Sun, X. D.; Wang, K. A.; Yoo, Y.; Wallace-Freedman, W. G.; Gao, C.; Schultz, P.G. *Adv. Mater.* 1997, 9, 1046-1049.
2. Moates, F. C.; Somani, M.; Annamalai, J.; Richardson, J. T.; Luss, D.; Wilson, R. C. *Ind. Eng. Chem. Res.* 1996, 35, 4801-4803.
3. Taylor, S.J.; Morken, J. P. *Science* 1998, 280, 267-270.
4. Wilson, R.C. *PCT Int. Appl.* 1997, 35 pp. CODEN: PIXXD2. WO9732208 A1 19970904.
5. Senkan, S. M. *Nature* 1998, 394, 350-353.
6. Cong, P.; Doolen, R. D.; Fan, Q.; Giaquinta, D. M.; Guan, S.; McFarland, E. W.; Poojary, D. M.; Self, K.; Turner, H. W.; Weinberg, W. H. *Angew. Chem. Int. Ed* 1999, 38, 484-488.
7. Cong, P.; Dehestani, A.; Giaquinta, D.; Guan, S.; Markov, D.; Self, K.; Turner, H.; and Weinberg H., *Proc. Natl. Aca. Sci.,* 1999, 96, 11077-11080.
8. Reddington, E.; Sapienza, A.; Gurau, B.; Viswanathan, R.; Sarangapani, S.; Smotkin, E. S.; Mallouk, T. E. *Science* 1998, 280, 1735-1737.
9. Miller, S. J.; Copeland, G. T. *J. Am. Chem. Soc.* 1999, 121, 4306-4307.
10. Su, H.; Yeung, E. S., *J. Am. Chem. Soc.,* 2000, 122, 7422-7423
11. Satsuma, A.; Hattori, A.; Mizutani, K.; Furuta, A.; Miyamoto, A.; Hattori, T. and Marukami, Y., *J. Phys. Chem.* 1998, 92, 6052-6058
12. Satsuma, A.; Hattori, A.; Mizutani, K.; Furuta, A.; Miyamoto, A.; Hattori, T. and Marukami, Y., *J. Phys. Chem.* 1989, 93, 1484-1490

13. Okada, F.; Satsuma, A.; Furuta, A.; Miyamoto, A.; Hattori, T. and Marukami, Y., *J. Phys. Chem.* 1990, 94, 5900-5908

14. Satsuma, A.; Okada, F.; Hattori, A.; Miyamoto, A.; Hattori, T. and Marukami, Y., *Appl. Cata.* 1991, 72, 295-310

FIGURE CAPTIONS

Figure 1. Experimental set up. L1, L2 and L3 are cylindrical lenses

Figure 2. (a) Laser excitation scheme

(b) Radiation distribution of laser beam before and after line generator

Figure 3. Flow cell reactor with a 3×5 library sitting in the middle

Figure 4. A 3×5 library

Figure 5. Catalytic performance of V-Sn-O binary system (library 1)

(a) Fluorescence screening

(b) Near IR thermography screening

(c) Activity (NQ) and total activity of the catalysts in library1

Figure 6. Catalytic performance of V-Ti-O binary system (library2)

(a) Fluorescence screening

(b) Near IR thermography screening

(c) Activity (NQ) and total activity of the catalysts in library2

Figure 7. Catalytic performance of V-Mo-O binary system (library3)

(a) Fluorescence screening

(b) Near IR thermography screening

(c) Activity (NQ) and total activity of the catalysts in library3

Figure 8. Catalytic performance of V-W-O binary system (library4)

(a) Fluorescence screening

(b) Near IR thermography screening

(c) Activity (NQ) and total activity of the catalysts in library4

Figure 9. Screening of catalytic activity for V-Sn-Mo-O catalysts

(a) Library 5, screening by fluorescence imaging (NQ)

(b) Library 5, screening by near IR thermography

(c) Library 6, screening by fluorescence imaging (NQ)

(d) Library 6, screening by near IR thermography

Figure10. Temperature dependency of catalytic activity (NQ), LIFI screening of V-Sn-Mo-O catalysts (library 5) at temperature of

(a) 603K

(b) 613K

(c) 623K

(e) 633K

(f) 643K

Figure 11. Temperature dependency of catalytic activity

Figure 12. Composition analysis of catalysts in library 3 by LA-ICP-MS

Figure 13. Calibration curve of LA-ICP-MS analysis

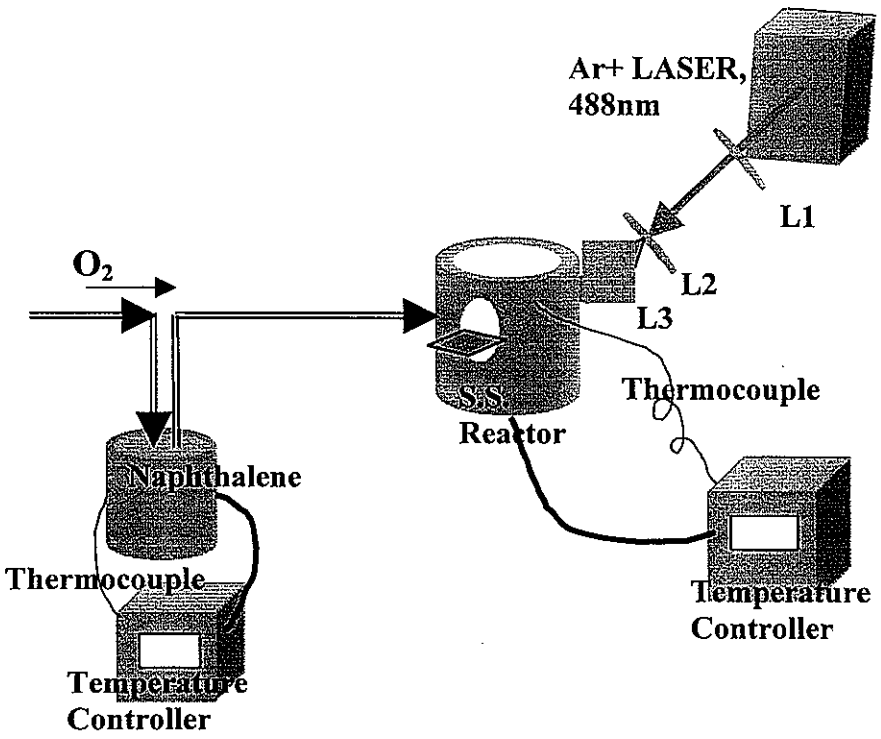
Ar+ LASER,
488nm
L1
L2
L3
O_2
S.S.
Reactor
Thermocouple
Naphthalene
Thermocouple
Temperature
Controller
Temperature
Controller

Figure 1

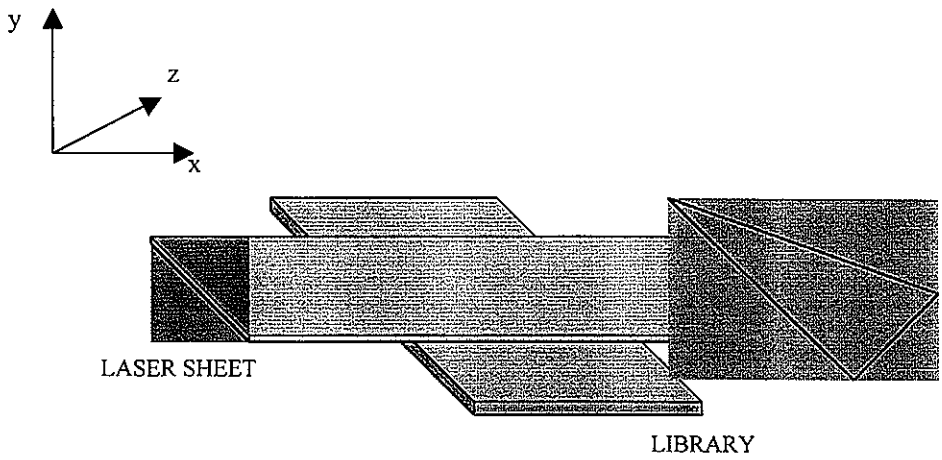
y
z
x
LASER SHEET
LIBRARY

(a)

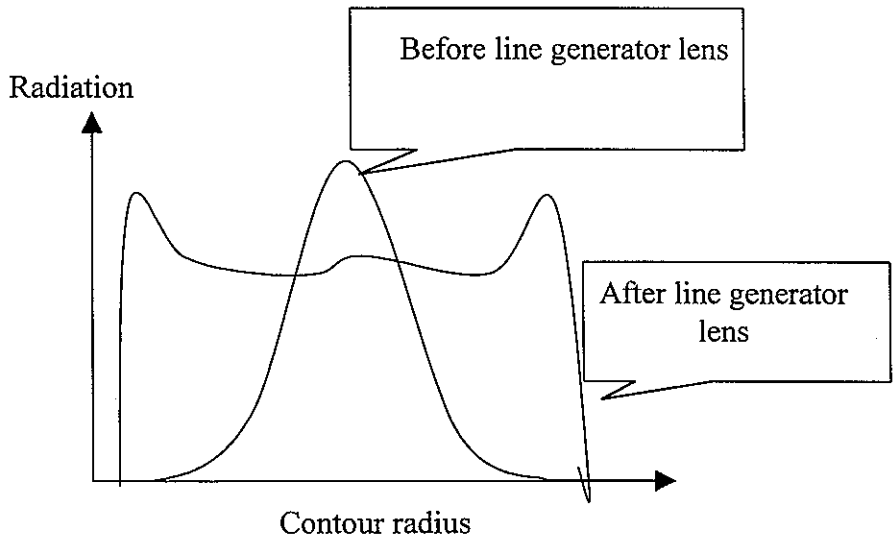
Radiation
Before line generator lens
After line generator lens
Contour radius

(b)

Figure 2

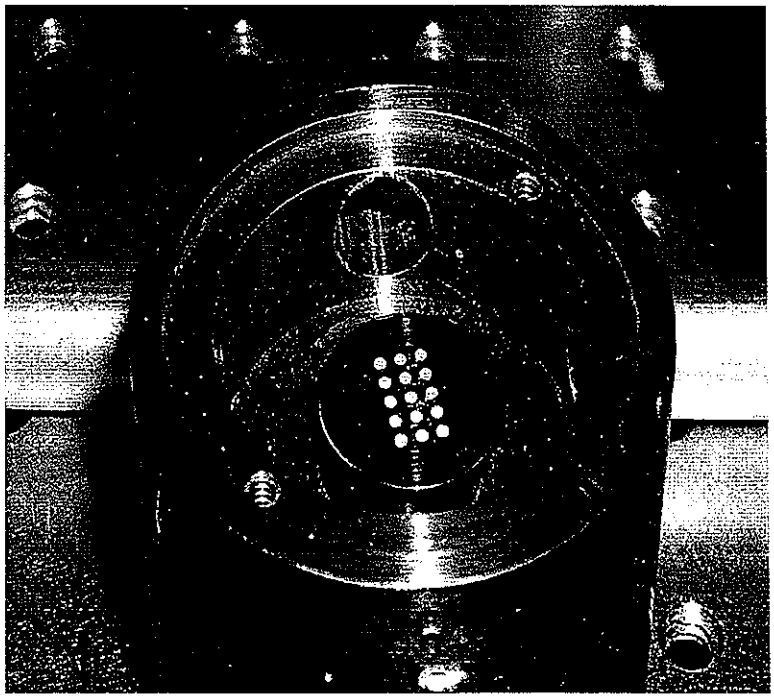

Figure 3

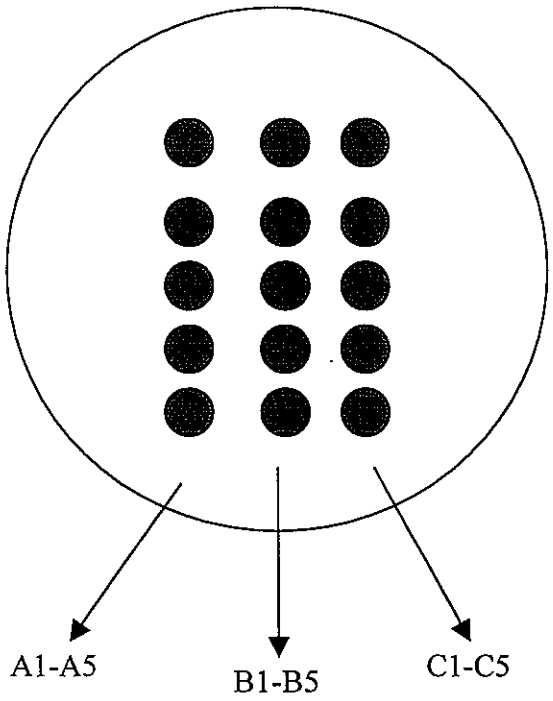

Figure 4

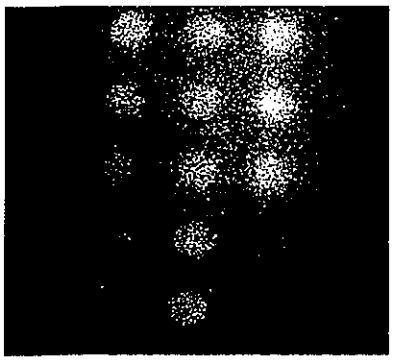

(a)

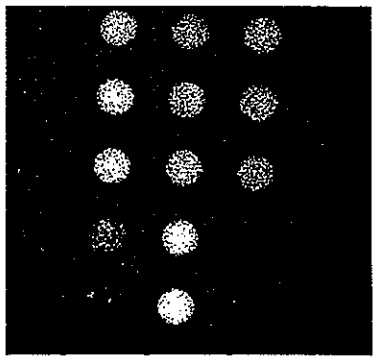

(b)

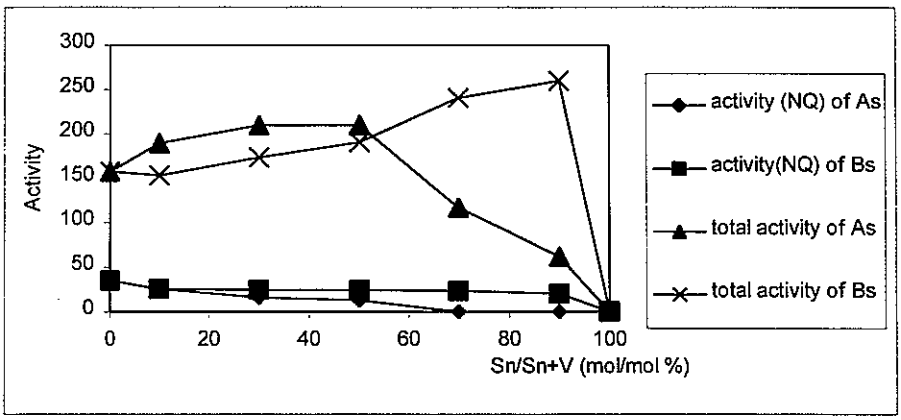
300
250
200
150
100
50
0
Activity
0
20
40
60
80
100
Sn/Sn+V (mol/mol %)
activity (NQ) of As
activity(NQ) of Bs
total activity of As
total activity of Bs

(c)

Figure 5

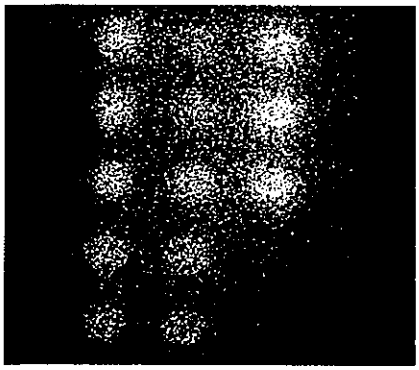

(a)

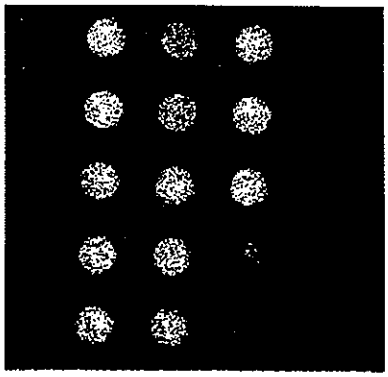

(b)

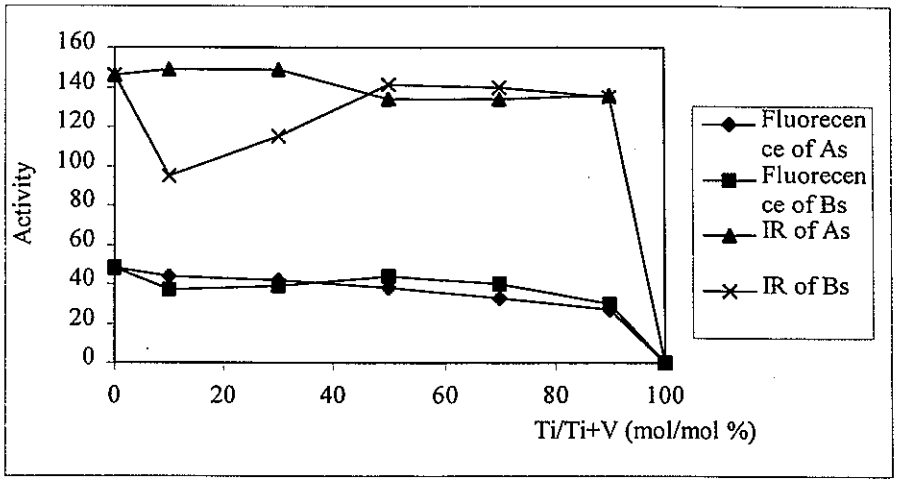
160
140
120
100
80
60
40
20
0
Activity
0
20
40
60
80
100
Ti/Ti+V (mol/mol %)
Fluorecen ce of As
Fluorecen ce of Bs
IR of As
IR of Bs

(c)

Figure 6

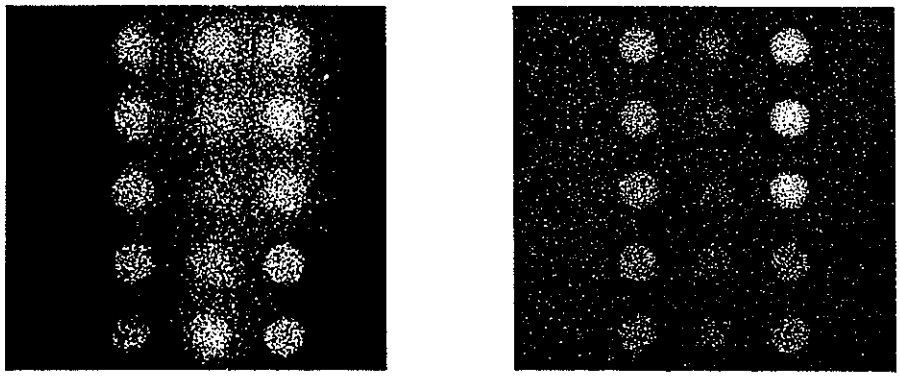

(a) (b)

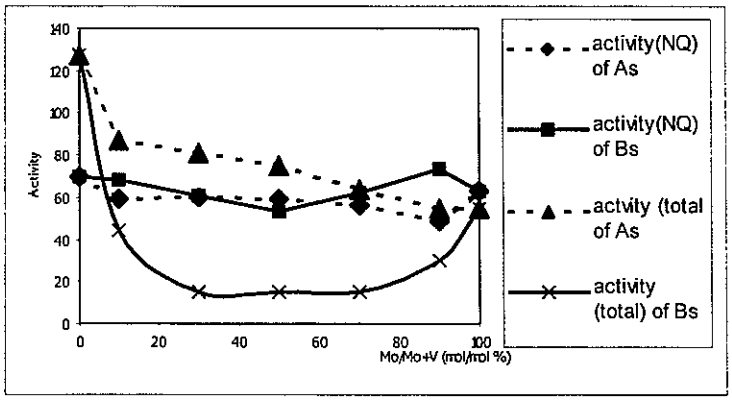
Activity
0
20
40
60
80
100
120
140
0
20
40
60
80
100
Mo/Mo+V (mol/mol %)
activity(NQ) of As
activity(NQ) of Bs
actvity (total of As
activity (total) of Bs

Figure 7

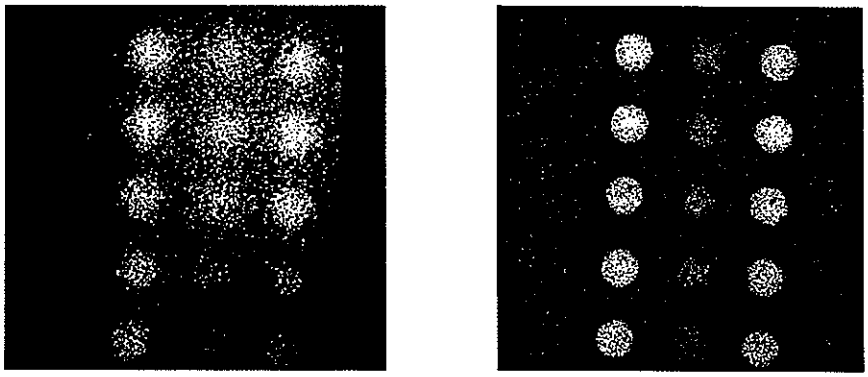

(a) (b)

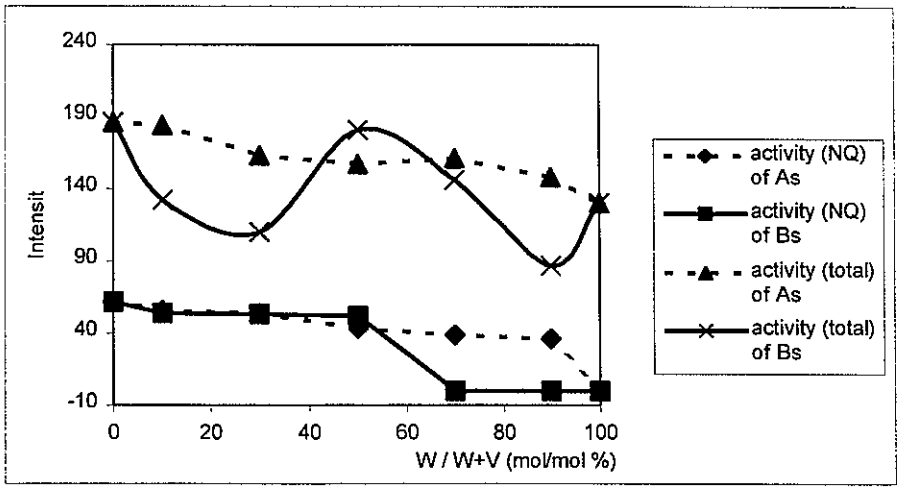
240
190
140
90
40
-10
Intensit
0
20
40
60
80
100
W / W+V (mol/mol %)
activity (NQ) of As
activity (NQ) of Bs
activity (total) of As
activity (total) of Bs

(c)

Figure 8

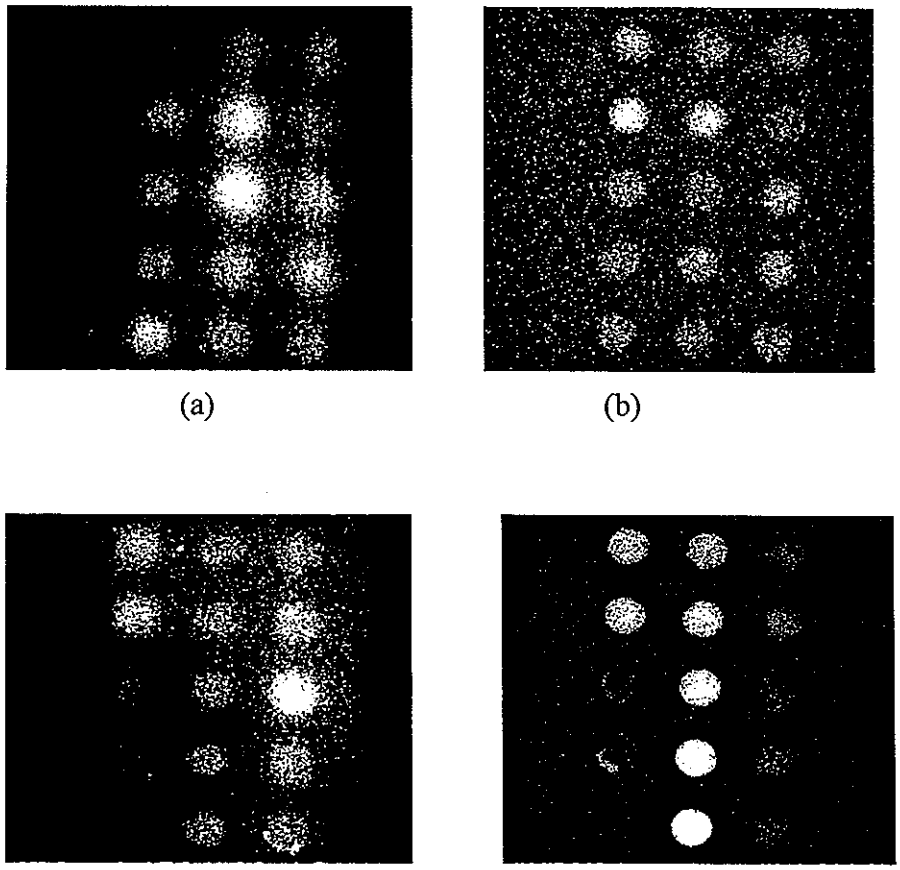

Figure 9

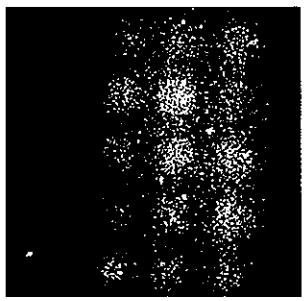

(a)

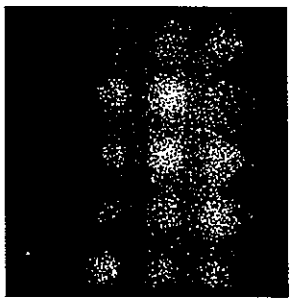

(b)

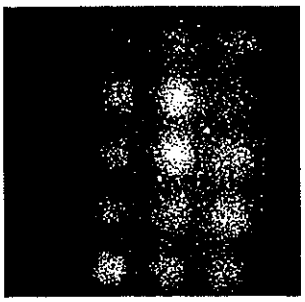

(c)

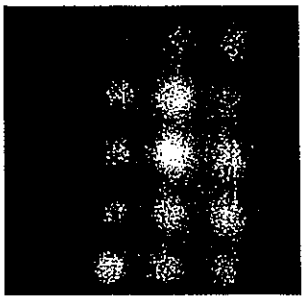

(d)

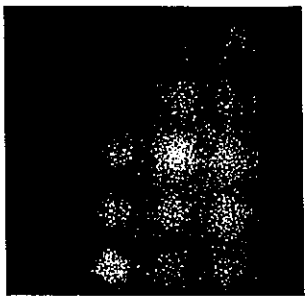

(e)

Figure 10

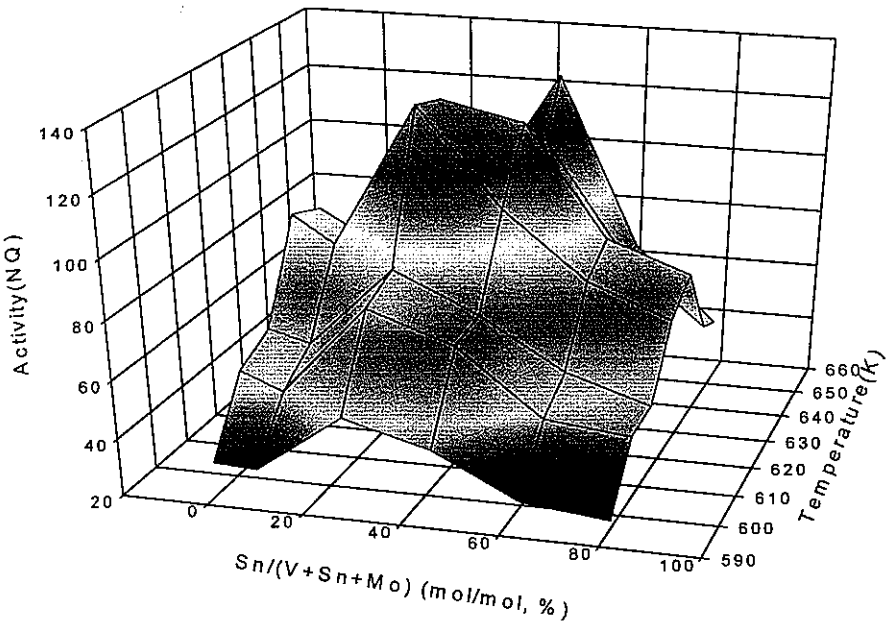
Activity(NQ)
140
120
100
80
60
40
20
0
20
40
60
80
100
Sn/(V+Sn+Mo) (mol/mol, %)
660
650
640
630
620
610
600
590
Temperature(K)

Figure 11

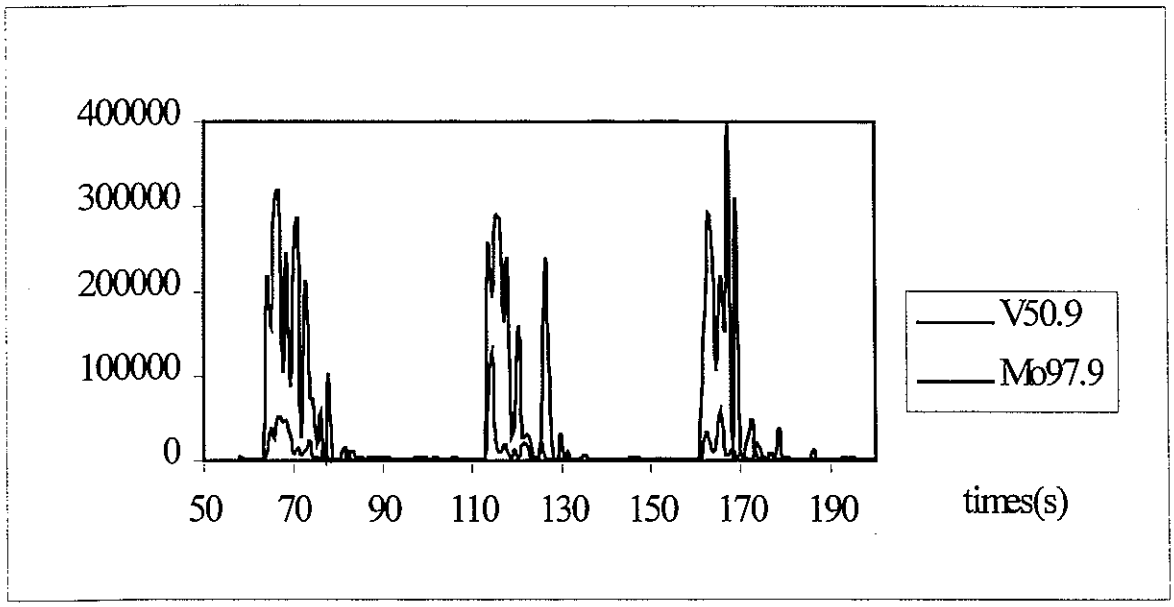
400000
300000
200000
100000
0
50
70
90
110
130
150
170
190
times(s)
V50.9
Mo97.9

Figure 12

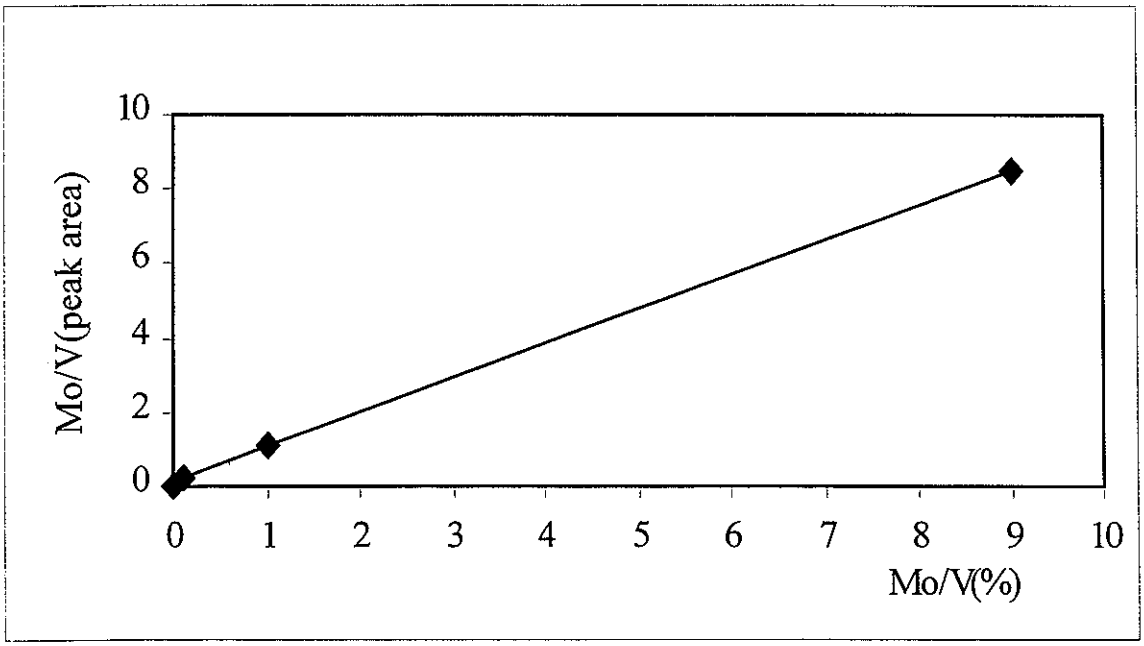

Figure 13

CHAPTER 4. COMBINATORIAL STUDY OF ZEOLITE IN CATALYZING ACYLATION OF BENZEN VIA LASER-INDUCED FLUORESCENCE IMAGING

A paper prepared for submission to Analytical Chemistry

Hui Su and Edwards S. Yeung

Abstract

Laser-induced Fluorescence Imaging (LIFI) has been developed into a High-throughput Screening (HTS) technique for heterogeneous catalysts, and it was used in discovering active oxidative catalysts. Here we demonstrate an application of LIFI in combinatorial study of zeolite catalytic system, it can accelerate not only the discovery process for heterogeneous catalysts, but also the optimization the reaction conditions as well as the catalytic process.

LIFI was used to simultaneously screen the catalytic properties of a 15-member library consisting mordenites (MOR), Ferrierites (FER), ZSM-5 (MFI), zeolite γ (FAU) and beta zeolites (BEA) with various Si/Al ratios in acylation of benzene with phthalic anhydride, and only beta zeolites were found active in this reaction at reaction temperature range of 190°C-340°C. Substantial deactivation of beta zeolites were observed in less than one minute at higher temperature, and the deactivation differed with reaction temperature, the

composition of reactant mixture as well as the Si/Al ratio of the beta zeolites. The deactivated beta zeolites can be regenerated partially by heating in oxygen flow. Up to 80% recovery of catalytic activity was obtained. Similar recovery was observed after numbers of deactivation-regeneration cycles.

Introduction

Driven by people's desire of discovery, combinatorial chemistry has achieved enormous success in drug discovery. Although the impact of combinatorial chemistry is less obvious in discovery of new solid-state materials, some promising works have been reported. The thin film solid-state library of 128 elements reported by Schultz and Xiang[1] for the first time demonstrated that the combinatorial approach could be used to discover solid-state materials with useful properties, super conductors in this case. Soon after their first success, Schultz and his co-workers announced the combinatorial discovery of a new class of magnetoresistive materials on their thin film libraries.[2] The success in combinatorial synthesis of solid-state materials library by thin-film technology soon was joined by liquid-phase synthesis and ink-jet technique.[3-5] On the other hand, high-throughput Screening (HTS) of solid-state libraries are much more complicated and less successful than combinatorial synthesis of solid-state libraries especially for the libraries of heterogeneous catalysts. Although high-throughput screening methods of heterogeneous catalysts by IR thermography, [6,7] laser-induced resonance-enhanced multi-photon ionization, [8] microprobe sampling mass spectrometry, [9] and fluorescence indicators[10, 11] have been reported, there are still a lot more to wonder in combinatorial screening of libraries of heterogeneous catalysts.

Recently we presented Laser-induced Fluorescence Imaging (LFI) as an alternative to high-throughput screening techniques for heterogeneous catalysts, [10] catalytic performance of a larger number of vanadium catalysts was screened simultaneously with sufficient spatial and time resolution under the real reaction conditions. Infrared imaging can also be performed in this instrumentation and more information can be withdrawn by performing both fluorescence and IR detection. We conducted a systematic study of vanadium catalysts in oxidation of naphthalene.[11] In our study, reaction condition and catalytic performance of a larger number of combinations of binary and ternary vanadium catalysts were screened by LIFI and some combinations have been found with much better catalytic performance than conventional catalyst, vanadium pentoxide, in oxidizing naphthalene to naphthoquinone; effects of various additives to the catalytic selectivity of vanadium pentoxide are studied by comparing the IR detection results and fluorescence results; coupled with laser ablation-ICP-MS, on-chip high throughput composition analysis can be achieved and combinations of solid catalysts with interests can be known without damaging the library.

Zeolites have been of intense interest as catalysts for some three decades because of the high activity and unusual selectivity they provide, mostly in a variety of acid-catalyzed reactions. Aromatic acylation is a very important practice in various areas of the fine chemicals industry. For instance many synthetic fragrance of the musk type contain an acetyl group, also the synthesis of several major pharmaceuticals (Ibuprofen, (s)-Naproxen) involve an aromatic acylation step. Conventional industrial practice generally use acid chlorides together with a stoichiometric amount of metal chloride, which means a high amount of inorganic by-product. Zeolites have been proven ideal substitute for metal chloride in these reactions with higher efficiency and selectivity and less waste. [15]

In catalysis, catalyst deactivation is one of the most concerned problems. For different catalysts, their stability in terms of activity and selectivity can last as long as years, some as short as seconds. Zeolites are the typical unstable but extremely useful heterogeneous catalytic system in industry, and carbonaceous deposits (coke) can deactivate Zeolites easily; the coke structure varies with conditions, but consists essentially of ill-defined poly-aromatic compounds. [12] Zeolite's catalytic stability period in oil cracking is about 1 minute.[13]

For an unstable catalytic system, a meaningful screening should provide information of catalytic activity as well as stability. Time resolution of a high-throughout screening technique plays a key role in this case. As we mentioned in our previous report that LIFI has good spatial resolution and detection limit as well as excellent time resolution (sub-micro seconds), which makes it a very good choice in combinatorial screening or study unstable heterogeneous catalysts.

In this work, the catalytic performance of a 15-member library consisting mordenites, Ferrierites, ZSM-5, zeolite γ and beta zeolites with various Si/Al ratios is screened in a high-throughput fashion by LIFI. The effects of structures, Si/Al ratio, reaction temperature and reactants on the catalytic properties of these catalysts can be revealed in minutes instead of days by conventional approach.

Experimental Section

Acylation of Benzene

Interaction of benzene (Bz) with phthalic anhydride (PhA) is an interesting object for investigation, both for scientific purpose and industrial application:

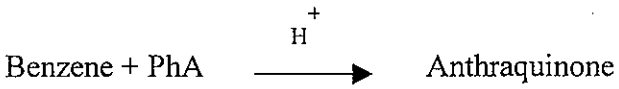

Zeolites are used to catalyze this reaction as solid acid from 190°C to 320°C at 1atm.

Catalyst Library

All zeolite samples were pretreated by heating at 550°C in O_2 flow for 5 hours. The catalyst libraries were constructed by depositing cyclohexane slurry of zeolites on sample plates. Sample arrangement is shown in figure 1. The zeolites on the 15-membered library are listed on table 1. The size of this library is 17mm diameter, and the diameter of individual catalyst site is 1mm. The amount of catalyst in each site on the library is about 100μg.

Reactants

All the zeolite catalysts were purchased from Zeolyst International (Valley Forge, PA). Benzene (99+%), cyclohexane (99+%) and phthalic anhydride (99+%) were obtained from Sigma (St. Louis, MO).

Instrumentation

The flow cell reactor and experimental setup of high throughput screening via LFI used in this work have been described elsewhere.[11] Solid phthalic anhydride (PhA) was melted in an oven and the vapor of PhA was fed into the flow reactor by nitrogen gas flow; benzene vapor was carried into reactor by bobbling nitrogen gas into liquid benzene (figure 2). The 488nm line of an Ar^+ laser (Coherent Laser Group, CA) was used to irradiate the region above the catalyst in a catalytic reaction, and the fluorescence intensity of a selected

product, anthraquinone, can be collected by a frame transfer CCD camera (Roper Scientific, NJ).

Results and Discussion

Zeolites in Acylation of Benzene

Zeolites with different structures behave differently in catalytic reactions. Side-by-side comparison of the catalytic behavior of different zeolites at the same time under the same reaction conditions would promise us accurate analysis and help us better understand the event. The zeolites of most interest in catalysis are those having medium to large pore sizes, consisting of 10- or 12- ring oxygen atoms, and having relatively high Si/AL ratio.[12] We prepared a 15-membered library consisting of consisting mordenites (MOR), Ferrierites (FER), ZSM-5 (MFI), zeolite γ (FAU) and beta zeolites in various Si/Al ratios, and screened their catalytic activities in acylation of benzene with PhA by monitoring the fluorescence intensity of the product, Anthraquinone, with LIFI in real reaction condition. Only β Zeolites were found to be active from reaction temperature range of 190°C – 340°C (figure 3), which agrees with previous report.[14] All the selected zeolite are well-characterized, and they all have relatively large pore sizes. The structure of MORs is a one-diemensional tube with an 8-ring pore structure; FERs and MFIs are of two-dimensional interconnecting structure with 8 or 10-ring; and FAU and Zeolite β have 3-dimensional network with 12-ring structure. Zeolite β is the only high-silica having a full three-dimensional network of 12-membered rings (table 1), which might explain its catalytic activity in reaction involving large aromatic molecules.

Si/Al ratio plays an important role in catalytic property of zeolite, but the effect of Si/Al on the catalytic performance of zeolites is somewhat unpredictable.[12] In our screening results of this library, we notice that the catalytic activity of zeolite β increases with its Si/Al ratio (figure 4). First, we have to consider the influence of Si/Al on acidity of zeolites because Zeolites act as acidic catalyst. In theory, for zeolites with same structure the activity of zeolite is somehow proportional to the number of aluminum atoms present. Lower Si/Al ratio, higher acidity, so higher activity should be expected; on the other hand, the concentrated acidic sites on the catalyst surface also promote the formation of polymeric species (coke) that hinders access to its inner surface, which depresses the catalytic ability of the catalyst. If the blocking effect of coke is dominant, higher acidic sites on the surface contribute to lower activity of the catalyst. In acylation of benzene with phthalic anhydride, the coke formed on the surface consists mainly polyaromatic that can cause serious blocking effect, which might explain the lower activity of lower Si/Al beta zeolites.

Reaction temperature is another critical element in catalytic reaction. The screening results of activities of four beta zeolites at temperature 190°C, 220°C, 250°C and 280°C are shown in figure 5. In this temperature range, increase of temperature causes the decrease of catalytic activity of beta zeolites in acylation of benzene. Similar results were reported in reference 14, and the decrease of catalytic activity is due to the selectivity change. The above screening results were obtained in 10 minutes by LIFI, which is at least 100 times (for 15 samples) faster than conventional testing approach by gas chromatography.

Deactivation of Zeolites

Zeolites can be deactivated by carbonaceous deposits (coke) that cover catalytic sites and block pores. Most coke formation is initiated by reactions on acid sites and therefore is also affected by their number and degree of acidity. In our experiment, beta zeolites started to deactivate in less than 1 minute at reaction temperature of 280°C (figure 6) while it was relatively stable at lower reaction temperature (<260°C). This is probably because either the coke formed at higher reaction is larger in size than that formed in lower temperature or the high temperature increase the production of coke. The stability of beta zeolites with various Si/Al ratios seems to experience similar effect caused by elevated temperature.

Since the deactivation of zeolites is related to coke formation, the composition of reactants might have influence on this process. We screened the catalytic activity of this library by LIFI at reaction temperature of 300°C with benzene/PhA of 0.8, 1.3 and 2.1. The screening results in figure 7 shows that beta zeolites deactivated faster at benzene /PhA of 2.1, which suggests that carbonaceous benzene ions are the main source of coke.

Regeneration of Deactivated Zeolites

Oxidizing the coke with air or oxygen at high temperature usually regenerates zeolite catalyst. There are some critical points that we need be clear for any regeneration process of catalyst: the regeneration time, the recovery and the number of regeneration cycles. One screen the catalytic reaction by LIFI will provide all these information for numbers of zeolites (or other catalysts), which cannot be done by conventional approach. At 300°C, beta zeolites were placed in reactor to catalyze the acylation of benzene for 2 minutes, and substantial deactivation was observed by LIFI; then oxygen instead of reactant mixtures was

introduced to regenerate the catalyst for 1s, 3s, 5s, 10s and 1 minute. 80% of recovery can be obtained after oxygen treatment for 3s. Lower recovery was observed at lower regeneration time, but increase of oxygen time beyond 3s will not increase the recovery of activity for deactivated zeolites. This suggests that the coke built up on zeolites can't be totally burnt up, or it changed the surface condition of zeolite in some ways. In order to study the efficiency of this regeneration process, we repeated the deactivation-regeneration cycles for number of times, similar recovery was obtained (figure 8).

Conclusion

Laser-induced Fluorescence Imaging (LIFI) has been successfully used in combinatorial study of beta zeolites in acylation of benzene with phthalic anhydride. The catalytic activity and stability of beta zeolites with different Si/Al ratio were screened by LIFI, and the comparison of these screening results help us better understand the catalytic mechanism. The regeneration process of deactivated beta zeolites was screened by LIFI, which provided the basic information in a high-throughput way to estimate a regeneration process and the value of these deactivated catalysts. For 15 samples, study the catalytic system by LIFI is up to 100 time faster than conventional testing, and higher throughput can achieved by using large library.

Acknowledgement

The Ames Laboratory is operated for the U.S. Department of Energy by Iowa State University under contract No. W-7405-Eng-82. This work was supported by the Director of Science, Office of Basic Energy Sciences, Division of Chemical Sciences.

References

1. X. D. Xiang; X. Sun; G. Briceno; Y. Lou; K. A. Wang; H. Chang; W. G. Wallace-Freedman; S. W. Chen; P. G. Schultz. *Science* 1995, 268, 1738-1740
2. G. Briceno; H. Chang; X. D. Sun; P. G. Schultz; X. D. Xiang. *Science* 1995, 270, 273-275
3. X. D. Sun; K. A. Wang; Y. Yoo; W. G. Wallace-Freedman; C. Gao; X. D. Xiang; P. G. Schultz. *Adv. Mater.* 1997, 9, 1046-1049
4. E. Reddington; A. Sapienza; B. Gurau; R. Viswanathan; S. Sarangapani; E. S. Smotkin; T. E. Mallouk. *Science* 1998, 280, 1735-1737
5. J. Klein; K. W. Lehmann; H. W. Schmidt; W. F. Maier. *Angew. Chem. Int. Ed.* 1998, 37, 3369-3372
6. F. C. Moates; M. Somani; J. Annamalai; J. T. Richardson; D. Luss; R. C. Wilson. *Ind. Eng. Chem. Res.* 1996, 35, 4801-4803
7. S. J. Taylor; J. P. Morken. *Science* 1998, 280, 267-270
8. S. M. Senkan. *Nature* 1998, 394, 350-353
9. P. Cong; R. D. Doolen; Q. Fan; D. M. Giaquinta; S. Guan; E. W. Mcfarland; D. M Poojary; K. Self; H. W. Turner; W. H. Weinberg. *Angew. Chem. Int. Ed.* 1999, 38, 484-488
10. H. Su; E. S. Yeung. *J. of Am. Chem. Soc.* 2000, 122, 7422-7423
11. H. Su; E. S. Yeung. *Analytical Chemistry*, submitted
12. C. N. Satterfield. *Heterogeneous Catalysis in Industrial Practice (2nd)*, McGraw-Hill, Inc., New York, 1991, p254

13. A. Brito-Alayon; R. Hughes; E.K.T. Kann. *Chem. Eng. Sci.* 1981, 36, 445

14. J. Weitkamp; H. G. Karge; H. Pfeifer; W. Hölderich, *Stud. Surf. Sci. catal.* 1994, 84 (Zeolites and Related Microporous Materials: State of the Art 1994), 1905-1912

15. H. van Bekkum; A. J. Hoefnagel; M. A. van Koten; E. A. Gunnewegh; A. H. G. Vogt; H. W. Kouwenhoven, *Stud. Surf. Sci. Catal.* 1994, 83 (Zeolites and Microporous Crystals), 379-390

TABLE CAPTIONS

Table 1. Zelites in the 15-membered library

Sample	Structure	Si/Al Ratio
Z1	zeolite γ	5
Z2	zeolite γ	30
Z3	zeolite γ	60
Z4	zeolite γ	80
Z5	zeolite β	25
Z6	zeolite β	75
Z7	zeolite β	150
Z8	zeolite β	300
Z9	Mordenite	20
Z10	Mordenite	90
Z11	ZSM-5	30
Z12	ZSM-5	80
Z13	ZSM-5	280
Z14	Ferrierite	20
Z15	Ferrierite	55

Table 1

FIGURE CAPTIONS

Figure 1. A 15-membered Library

Figure 2. Experimental Instrumentation

Figure 3. Activity Screening of A 15-membered Library by LIFI at Reaction Temperature of 190°C in Acylation of Benzene

Figure 4. Effect of Si/Al ratio on Catalytic Activity of Beta Zeolites

Figure 5. Catalytic Properties of Beta Zeolites at Different Temperatures

Figure 6. Deactivation of Beta Zeolites

(a) t = 3s

(b) t = 6s

(c) t = 9s

(d) t = 120s

Figure 7. The Effect of Benzene/PhA on Deactivation of Zeolites

Figure 8. The Regeneration of Deactivated Beta Zeolites in Oxygen Flow

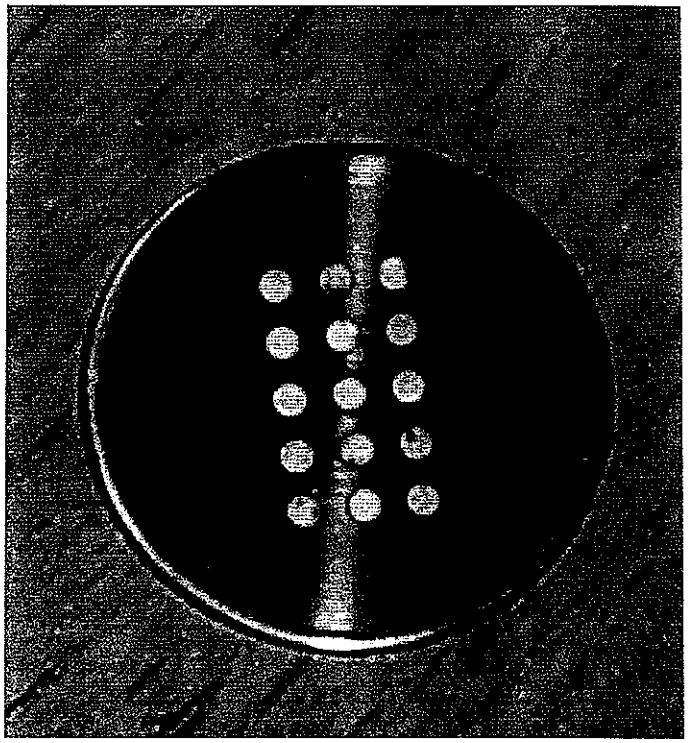

Sample Arrangement

Z1	Z5	Z9
Z2	Z6	Z10
Z3	Z7	Z14
Z4	Z8	Z15
Z11	Z12	Z13

Figure 1

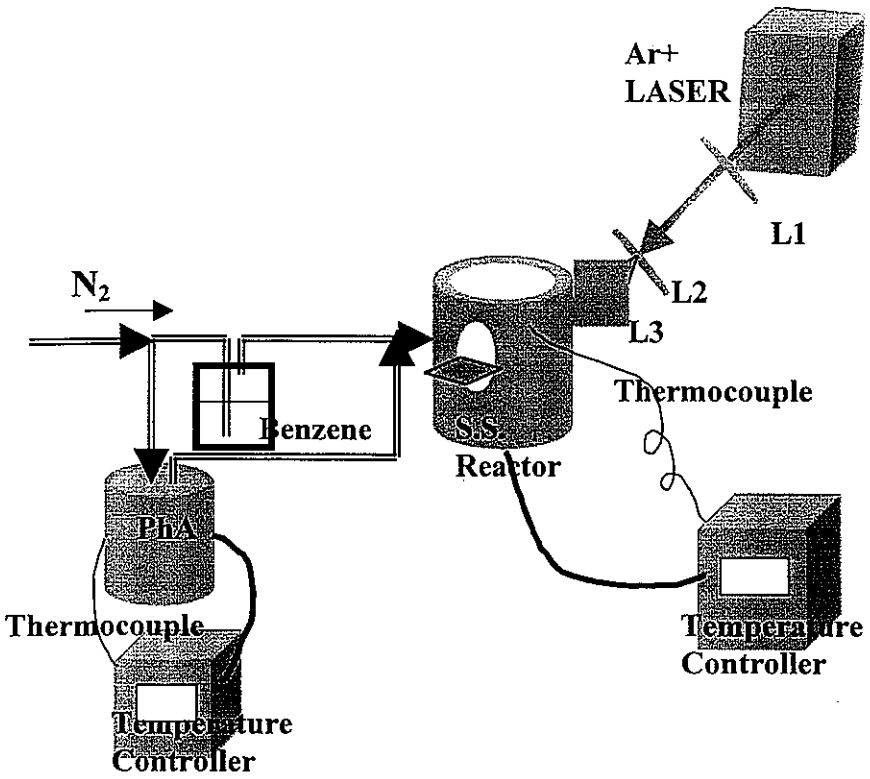
Ar+
LASER
L1
L2
L3
N_2
Thermocouple
Benzene
S.S.
Reactor
PhA
Thermocouple
Temperature
Controller
Temperature
Controller

Figure 2

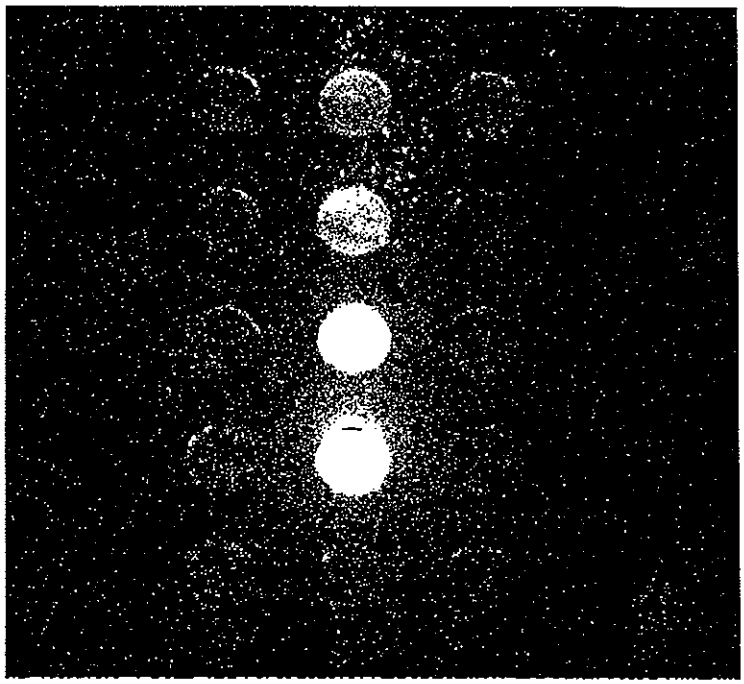

Figure 3

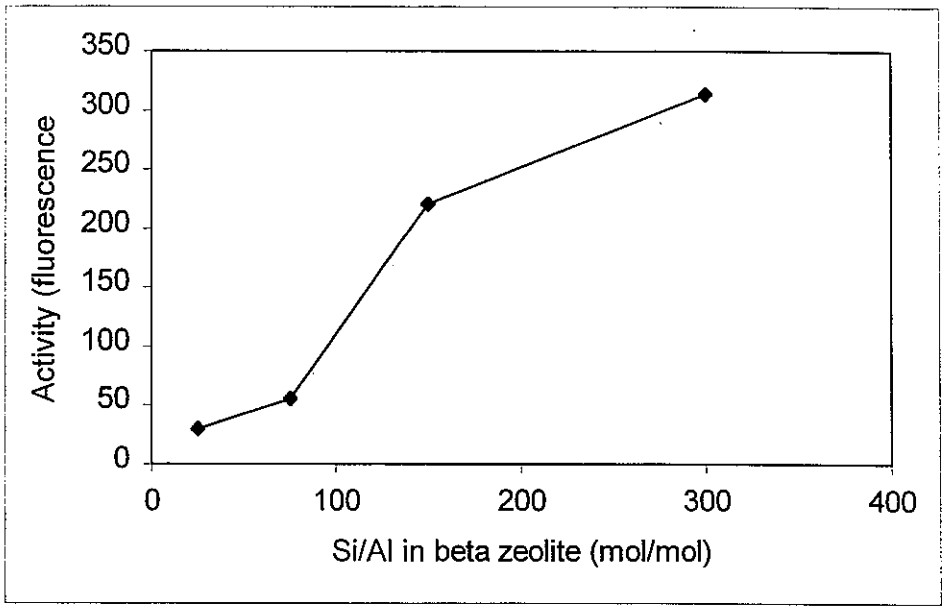
350
300
250
200
150
100
50
0
Activity (fluorescence
0
100
200
300
400
Si/Al in beta zeolite (mol/mol)

Figure 4

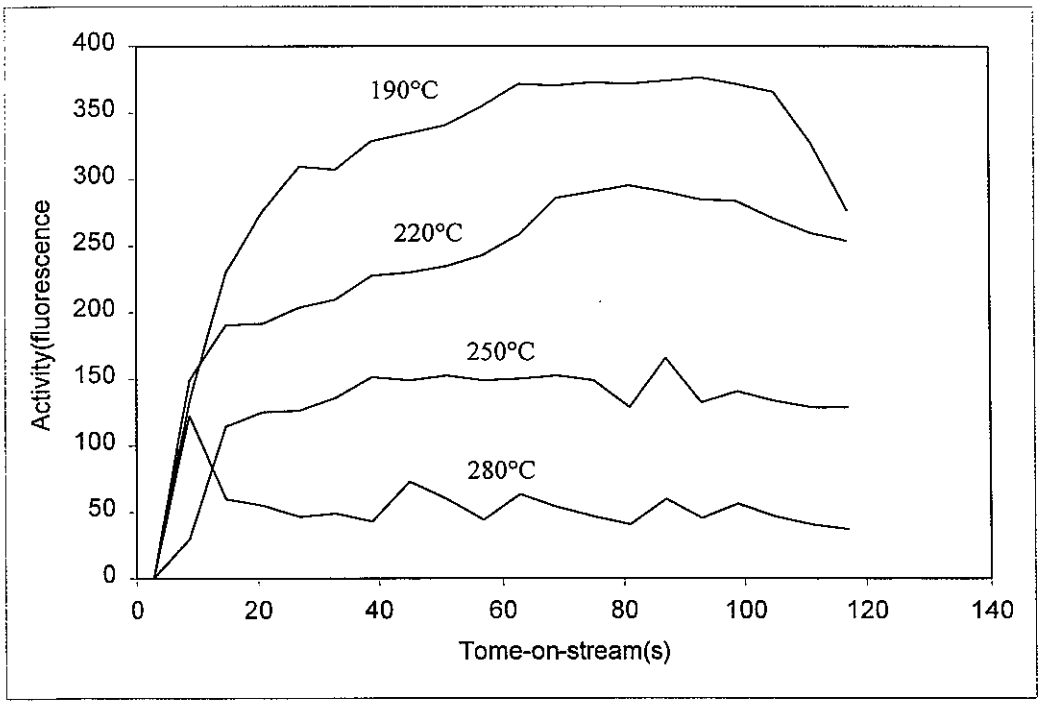
400
350
300
250
200
150
100
50
0
Activity(fluorescence
190°C
220°C
250°C
280°C
0
20
40
60
80
100
120
140
Tome-on-stream(s)

Figure 5

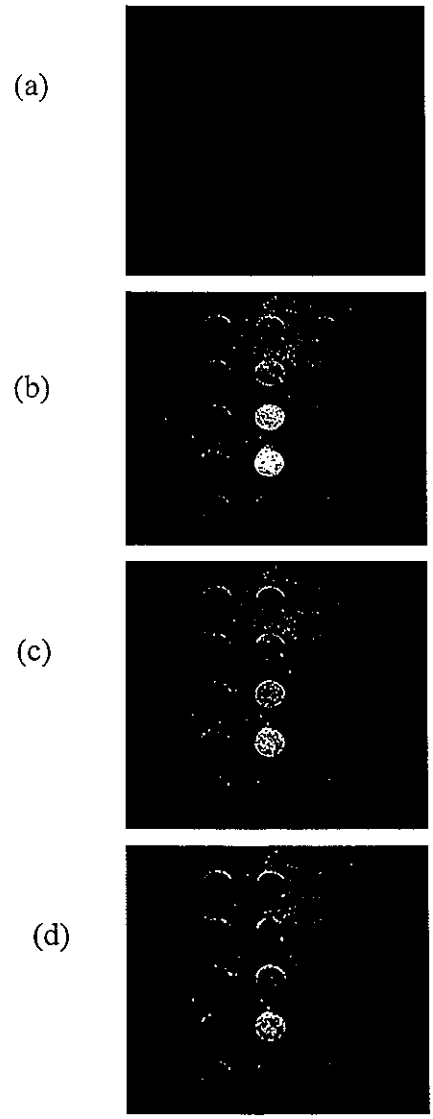

Figure 6

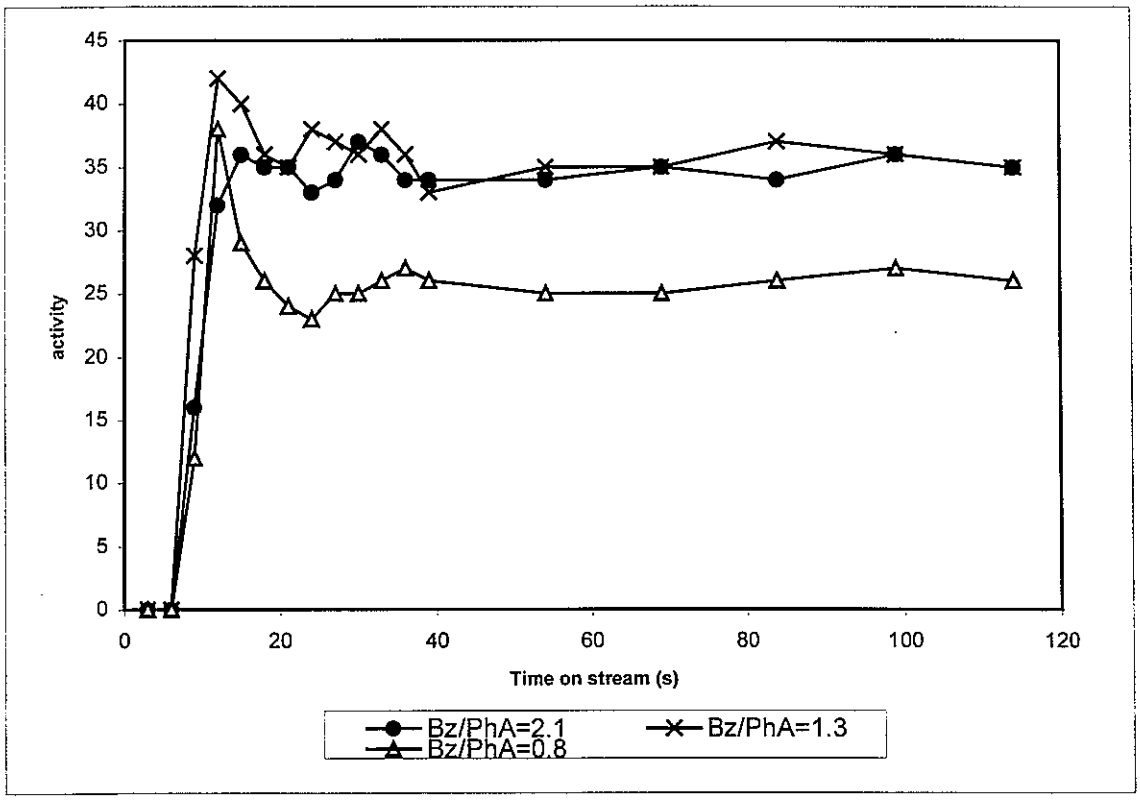
45
40
35
30
25
20
15
10
5
0
activity
0
20
40
60
80
100
120
Time on stream (s)
Bz/PhA=2.1
Bz/PhA=1.3
Bz/PhA=0.8

Figure 7

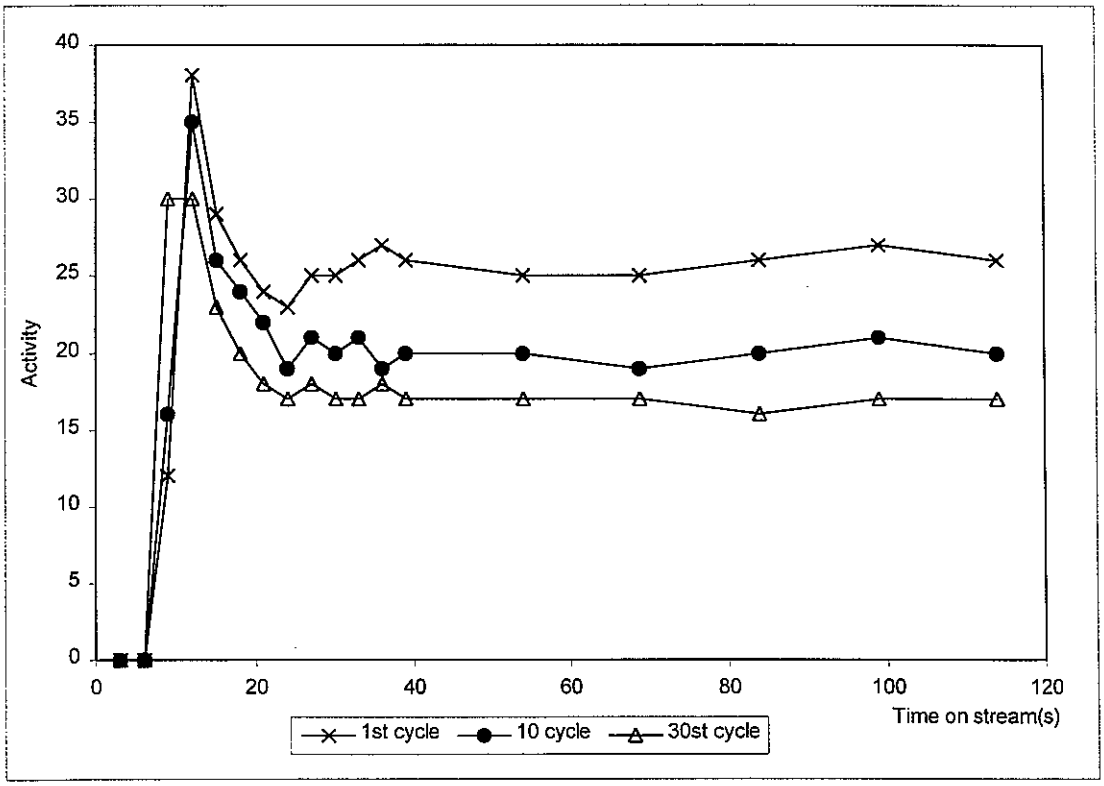
40
35
30
25
20
15
10
5
0
Activity
0
20
40
60
80
100
120
Time on stream(s)
1st cycle
10 cycle
30st cycle

Figure 8

PART 2. STUDY OF SINGLE CELL DEGRANULATION

CHAPTER 5. STUDY OF CELL DEGRANULATION WITH SIMULTANEOUS MICROSCOPE IMAGING AND CAPILLARY ELECTROPHORESIS

A paper published in Applied Spectroscopy

Hui Su and Edward S. Yeung

Abstract

The physical release of single granules from individual rat peritoneal mast cells (RPMCs) was monitored by video recording of the degranulating cells by a high-resolution CCD microscope system. The bright granular core disappears from the image as the vesicular content is dissolved on contact with the extracellular fluid. After a fixed time delay, the exocytotic product, serotonin, was detected by capillary electrophoresis coupled with laser-induced native fluorescence (CE-LINF). The timing of the two events are mostly correlated, which supports a fast release mechanism of the granular products.

Introduction

The cell is the fundamental unit of life. Studying the chemistry of dynamic cellular processes should allow us to better understand cellular functions. Capillary electrophoresis as a microscale analytical technique has been used in various chemical characterizations of single cells with electrochemical [1-3] or laser induced fluorescence (LIF) detection [4-6]. In

previous studies in our research group, the native fluorescence of various chemical species released from mammalian cells, such as catecholamines and proteins, has been utilized for detection. The temporal evolution of on-column exocytotic release of serotonin and proteins from individual rat peritoneal mast cells (RPMCs) was monitored by using laser-induced native fluorescence CE (LINF-CE) [5]. Events that are consistent with released serotonin from single granules were observed. Even higher temporal resolution of the dynamic release of serotonin from individual granules within RPMCs has been obtained with fast CE [6]. The study of exocytosis from RPMCs with native fluorescence imaging microscopy provided further information on this cellular process temporally and spatially [7].

It is known that serotonin and histamine are bound in a protein matrix inside granules that are surrounded by a vesicular membrane. When the granular core is expelled from the cell via exocytosis, the surrounding liquid (extracellular fluid) presumably solubilizes the granular contents to release the components. Electrochemical studies of single exocytotic events have been reported [8-10]. Optical images of the exocytotic events can be readily obtained by microscopy [5,11-13]. However, such optical observations have not been directly correlated with any of the above-mentioned chemical measurements. Rather, the number and the rate of exocytotic events were found to be similar in separate cells on consecutive chemical and physical (optical) interrogations. The amount of material detected per event was also consistent with the expected contents in single granules. Questions remain as to whether solubilization of the granular core is instantaneous, whether exocytosis can eject granules with the vesicular membrane intact, whether granules can fuse with each other before being ejected, and whether the vesicular membrane can fuse with the cell membrane internally to release the components inside the cytoplasm. Exploring the temporal

correlation between the physical release of granules and the chemical release of granular products in individual cells should be helpful for elucidating the mechanism. In the present work, we used a high-resolution CCD microscope system to monitor a degranulating mast cell trapped inside a capillary column. After a well defined time delay, the released serotonin, one of the granular products, was detected with LINF-CE. We were therefore able to follow each exocytotic event with unprecedented detail.

Experimental Section

Instrumentation

The experimental setup of CE-LINF detection used in this work has been described elsewhere [14]. A 21-μm I.D., 145-μm O.D. bare fused-silica capillary (Polymicro Technologies, Phoenix, AZ) was used, with a total length of 28 cm (14 cm to the detection window). A high-voltage supply (Glassman High Voltage Inc., Whitehorse Station, NJ) was used to drive the electrophoresis. Each new capillary was rinsed by pumping through deionized water, 20 mM NaOH, methanol, and buffer (2 min each) before use.

The 275.4 nm line of an argon ion laser (Model 2045, Spectra Physics, Mountain View, CA) was isolated with a prism and focused with a 1-cm quartz lens onto the detection window of the capillary as the excitation source. Fluorescence was collected with a 10× quartz microscope objective (Carl Zeiss, Germany) and passed through two UG-1 color filters (Schott Glass) onto a photomultiplier tube. Electropherograms were recorded at 10 Hz with a 24-bit A/D interface (ChromPerfect Direct, Justice Innovation, Palo Alto, CA) and were stored in a computer.

An Olympus CK-2 inverted microscope (Olympus Optical Co., Tokyo, Japan) was

used for all the imaging work and for monitoring single-cell injection. A CCD video camera (Model XC-73, Sony, Japan) was attached to the microscope to image cell degranulation at a rate of 4 frame/s. A video grabber (Smart Video Recorder Pro, Intel Co., Hillsboro, OR) was used to record the videos in a computer (Dell XPSM200).

Reagents

Mast cell Ringer buffer (MCR) was used as the cell suspension solution. MCR was prepared by dissolving 5 mM glucose, 5 mM $MgCl_2$, 2 mM $CaCl_2$, 2.5 mM KCl, 140 mM NaCl and 10 mM HEPES (Fisher Scientific, Fair Lawn, NJ) in deionized water (Milli-Q and Elix5, Millipore, Bedford, MA), and adjusted to pH 7.4. All solutions were filtered with a 0.22-μm cutoff cellulose acetate filter (Costar, Cambridge, MA) before use. Serotonin hydrochloride standard (Sigma Chemical, St. Louis, and MO) was dissolved in MCR to establish the detection limit. Polymyxin B sulfate (Pmx) (Life Technologies, Grand Island, NY) was dissolved in DMSO and diluted to strength in MCR. Isolation of rat peritoneal mast cells (RPMCs) was based on the method of Parpura and Fernandez [15]. Mast cells were harvested by peritoneal lavage from male Sprague-Dawley rats (Laboratory Animal Resources, Iowa State University, Ames, IA). The rats were anesthetized and then decapitated. Approximately 50 mL of lavage saline consisting of CO_2-independent medium (Gibco, Gaithersburg, MD) containing 0.175% fatty-acid-free bovine serum albumin (ICN Biomedicals, Costa Mesa, CA) was injected into the peritoneal cavity. The rat was inverted and massaged for 5 min. An incision was made into the cavity and the lavage saline was withdrawn. The lavage was centrifuged for 10 min (700 rpm, full brake, 10C). The pellet was resuspended in 1 mL of fresh lavage saline and layered over 2 mL of 0.22% metrizamide

(dissolved in the lavage saline). After a 20-min centrifugation (1400 rpm, no brake, 10C), the supernatant was discarded. The remaining pellet was resuspended and centrifuged for 10 min (700 rpm, full brake, 10C). The cell pellet was suspended in the lavage saline until use. Before cell injection the cells were washed twice in MCR and suspended in MCR.

Capillary electrophoresis

The procedure for injecting individual cells is the same as described previously [14]. A small drop of cell solution was placed on a microscope slide into which the inlet end of the capillary was inserted. About 5 mm of the polyimide coating at the injection end of the capillary was removed to allow visual observation of cell injection and subsequent video recording of the degranulation of single cells by the CCD camera. One cell can be injected into the capillary tip by applying suction with a syringe and the process can be visually confirmed through the microscope. The cell solution was then wiped away and the microscope slide was replaced by a clean one. A large liquid drop (about 200 μL) of Pmx in diluted MCR (33% in water) was added to the slide. Electrophoresis was driven at 9 kV for several minutes to transport the released serotonin derived from degranulation of the cell to the detection window. The CCD camera records the optical images of the mast cell in the capillary as soon as high voltage was applied to the capillary.

Results and Discussion

Imaging the morphological changes of mast cells is how one can study the physical release of granules from individual cells after stimulation by Pmx. Intact mast cells are round with a smooth and well-defined cell membrane when maintained in their native

environment. Morphology changes can be triggered by many events besides degranulation, such as heat, electric field and pH. Since we are studying cell degranulation under high-speed capillary electrophoresis conditions, the effects of Joule heating and high electric field must be considered. A high electric field gradient provides fast transport of the components released by the cell and improves the temporal resolution of exocytotic events [6]. However, it might also cause significant Joule heating and damage the cells because of the high ionic strength (150 mM) of the MCR buffer. We found that the morphology of cells trapped in the capillary dramatically changed right after 12 kV was applied to the capillary even in the absence of Pmx. No useful information can be obtained by studying the degranulation of such damaged cells. These undesirable heating effects can be controlled by using diluted MCR solution as the CE buffer and by lowering the high voltage. Under our experimental conditions, the mast cells appear to remain viable under the microscope (40×) with electrophoretic currents lower than 20 μA. So, we limited the operating current to below 15 μA (9 kV was applied), which still provides reasonable temporal resolution.

When a cell is injected by suction, a plug of cell suspension solution, diluted MCR, is injected with it at the same time. This keeps the cell in the environment of reasonable ionic strength until the initiation of electrophoresis. Mast cells tend to adhere to the capillary surface, which makes on-column single-cells analysis possible. However, it still takes some time for a cell to stabilize inside the capillary after the high voltage is applied. This is likely the result of shear force induced by electroosmotic flow or a change in surface charge from the axial electric field. For different cells, the situations are different. Some cells fluctuate for a few seconds and some move a short distance along the direction of electroosmosis before becoming stationary. This issue must be considered when interpreting the images of

degranulating cells, *vide infra.*

The concentration of secretagogue plays an important role in the degranulation of RPMCs. A higher concentration of Pmx causes faster cell degranulation and increases the amount of released material. Figure 1a and b are electropherograms of serotonin released from two single cells under the same experimental conditions except for the strength of Pmx. Earlier appearance of the first exocytotic event and more violent release of serotonin are associated with a higher concentration of Pmx in Fig. 1b. There, the individual events are barely separated from each other. On the other hand, less stimulation seems to delay and slow down the rate of degranulation. The delay of exocytotic events also depends on the physical state of the cells. Finally, the presence of Pmx can increase the retention time of serotonin by reducing electroosmotic flow. The experimental conditions must therefore be tightly controlled.

In order to establish the correlation between cell degranulation and the release of chemical species, we have to analyze the cell images with care. Since we monitored cell degranulation under a microscope with high resolution, individual granules can be seen as bright spots emerging from the cell membrane. Subtracting these images consecutively should provide a movie of granule release, because the disappearance of a granule results in a negative subtraction. That is, a dark spot should appear on the subtracted image at the very location this event occurs. The first two images in Figure 2a are consecutive images of a degranulating mast cell chosen from a video record at 4 frames/s. It is difficult to visually identify any changes that may have occurred. The corresponding subtracted image is shown on the right hand side. The disappearance of one granule is clearly depicted as the dark spot on the subtracted image. We note however that movement of granules or the entire cell in

the capillary can also contribute to light intensity changes and bring negative subtraction results. In the case of movement of a granule, a black spot (negative subtraction result) at the previous position should be present next to a bright spot (positive subtraction result) at the new position. This is evident in the series of images in Fig. 2b. This way, we can distinguish between granular release events and movement.

By counting the granular events on the subtracted images over the entire video record, a time dependent digital granule-release plot can be obtained as in Figure 3a. While the images of the degranulating mast cell were being recorded, the released serotonin was detected by LINF-CE simultaneously, as shown in the electropherogram in Fig. 3b. As noted in previous work [5], proteins and histamine are also released on degranulation. Proteins migrate much slower under electrophoresis and will not appear within the time span of Fig. 3b. Histamine does not absorb or fluoresce at these wavelengths. The first detectable signal in the electropherogram appeared around 3.7 min after the injection of Pmx. The appearance time is actually around 2.4 min since one must correct for the electrophoretic migration time of serotonin of 1.3 min. The release events lasted about 2 min for this cell.

The comparison of the physical release of granules and the chemical release of serotonin is shown in Figure 3. The amount of granular products being released is different from granule to granule, which means that some of the serotonin peaks may be below the detection limit and are not detected. The video images also do not register every de-granulation event due to limited depth of field and opacity of the cell. Considering these experimental limitations, there is reasonably good temporal match between Fig. 3a and b except for the region before the major release activity at 630 frames. Since in most cases serotonin was detected right after the granule was released and dissolved (disappeared), a fast

release mechanism of granular product can be concluded.

However, there are also some uncorrelated peaks in Fig. 3, implying that not every granule dissolves and releases its core products immediately. Occasionally, we can observe single granules move away from the cell without being dissolved [7]. This will lead to uncorrelated peaks. The degranulation of mast cells has been found to be incomplete [6]. This incomplete process might be because multiple stages of the cell degranulation exist for the physical release of granules and serotonin release. The fast and incomplete degranulation is possibly due to an equilibrium process, which supports the assumption of an ion exchange mechanism for the storage and release of cationic secretory products [16].

Conclusions

Based on the good temporal correlation with events observed through an optical microscope, we have identified individual peaks in the fluorescence electropherograms as serotonin released from the granular core on contact with the surrounding fluid. The distribution of peak sizes implies that the granules contain different amounts of serotonin. In most cases, release is instantaneous and is localized to the cell surface. In rare cases, granules are transported away from the cell intact, resulting in delayed release or no release at all.

Acknowledgement

The Ames Laboratory is operated for the U.S. Department of Energy by Iowa State University under Contract No. W-7405-Eng-82. This work was supported by the Director of Energy Research, Office of Basic Energy Sciences, Division of Chemical Sciences.

References

1. A. G. Ewing, J. M. Mesaro and D. F. Gavin, Anal. Chem., *66*, 527A (1994).
2. H. K. Kristensen, Y. Y. Lau and A. G. Ewing, J. Neurosci. Methods, *51*, 183 (1994).
3. A. G. Ewing, J. Neurosci. Methods, *48*, 215 (1993).
4. H. T. Chang and E. S. Yeung, Anal. Chem., *67*, 1079 (1995).
5. S. J. Lillard and E. S. Yeung, Anal. Chem., *68*, 2897 (1996).
6. A. Ho and E. S. Yeung, J. Chromatogr. A, *817*, 377 (1998).
7. S. J. Lillard and E. S. Yeung, J. Neurosci. Methods, *75*, 103 (1997).
8. A. F. Oberhauser, I. M. Robinson and J. M. Fernandez, Biophys. J., *71*, 1131 (1996).
9. K. Pihel, H. Showchien, J. W. Jorgenson and R. M. Wightman, Anal. Chem., *67*, 4514 (1995).
10. K. Pihel, E. R. Travis, R. Borges and R. M. Wightman, Biophys. J., *71*, 1633 (1996).
11. C. Bronner, Y. Landry, P. Fonteneau and J-G. Kuhry, Biochem., *25*, 2149 (1986).
12. J. H. Phillips, K. Burridge, S. P. Wilson and N. Kirshner, J. Cell Biol., *97*, 1906 (1983).
13. S. Maiti, J. B. Shear, R. M. Williams, W. R. Zipfel and W. W. Webb, Science, *275*, 530 (1997).
14. B. L. Hogan and E. S. Yeung, Anal. Chem., *64*, 2841 (1992).
15. V. Parpura and J. Fernandez, Biophy. J., *71*, 2356 (1996).
16. B. Uvnas and C-H. Aborg, News Physiol. Sci., *4*, 68 (1989).

FIGURE CAPTIONS

Figure 1. Electropherograms of serotonin released from single mast cells stimulated by (a) Pmx at 40 U and (b) Pmx at 200 U.

Figure 2. Original (left) images and subtracted (middle) images of degranulating mast cells in the capillary. (a) t1 = 186.00 s, t2 = 186.25 s and the net change(right), and (b) t1 = 26.75 s, t2 = 27.00 s and the net change (right),

Figure 3. Comparison of (a) the discrete count of physical release of granules and (b) the amounts of released serotonin during the degranulation. Each frame corresponds to 0.25 s. Physical release events were identified from subtracted images similar to those in Figure 2 and have been time-shifted by 1.3 min to account for the electromigration of serotonin to the fluorescence detector.

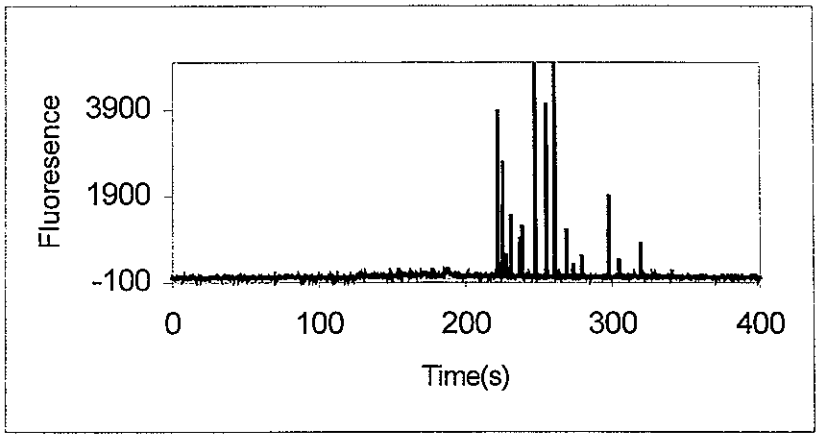
Fluoresence
3900
1900
-100
0
100
200
300
400
Time(s)

(a)

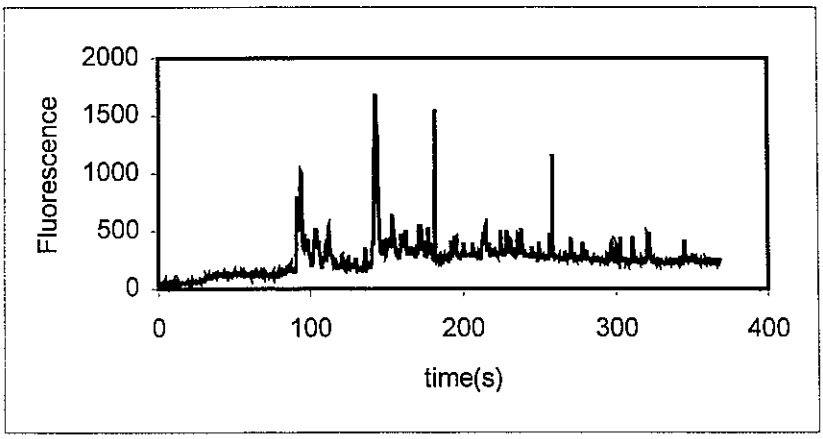
Fluorescence
2000
1500
1000
500
0
0
100
200
300
400
time(s)

(b)

Figure 1

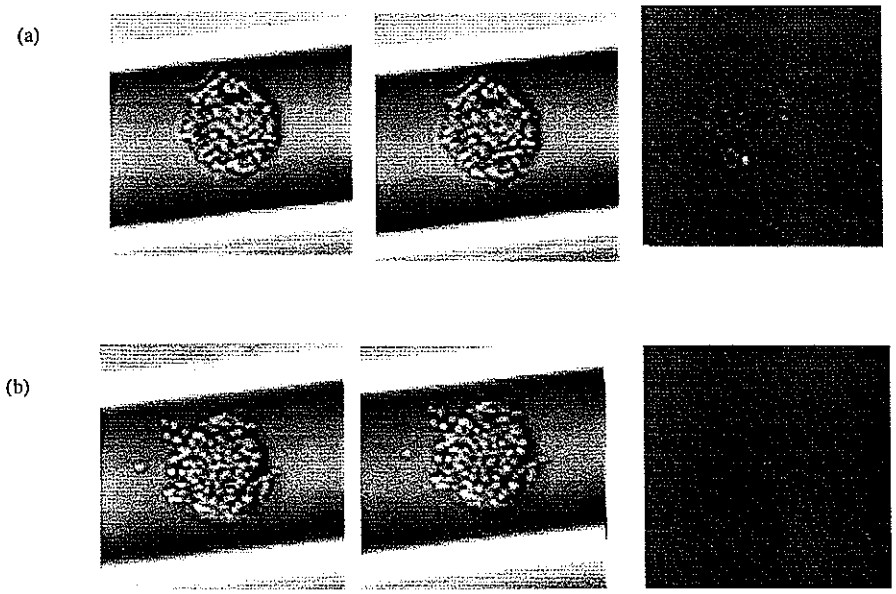

Figure 2

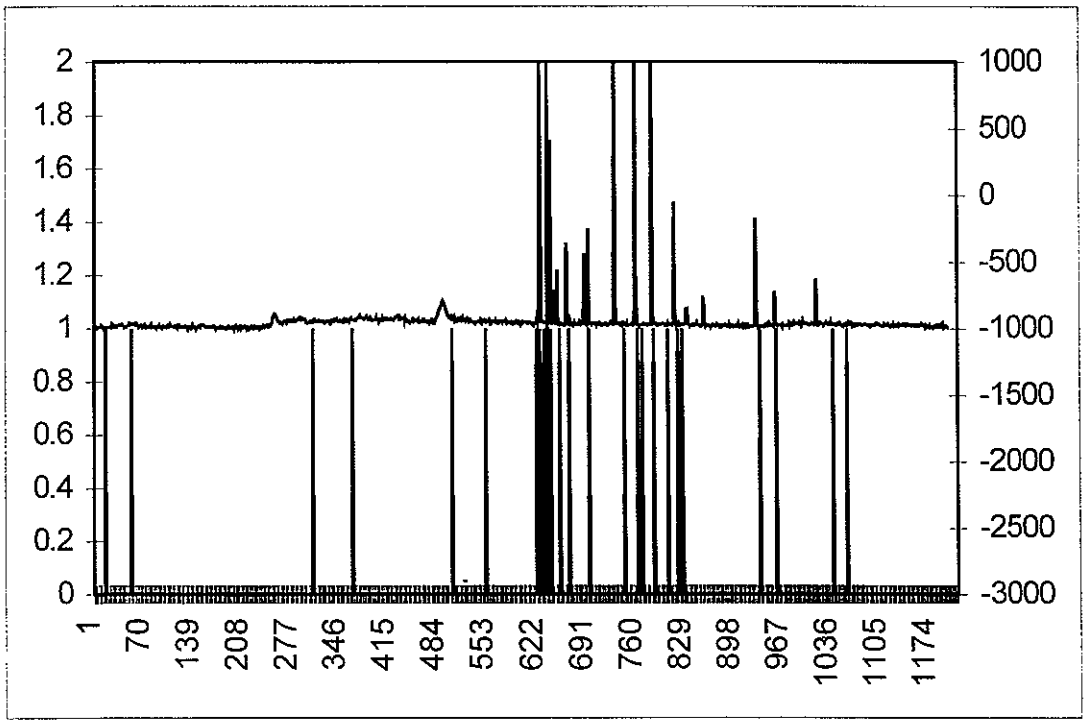
2
1.8
1.6
1.4
1.2
1
0.8
0.6
0.4
0.2
0
1000
500
0
-500
-1000
-1500
-2000
-2500
-3000
1
70
139
208
277
346
415
484
553
622
691
760
829
898
967
1036
1105
1174

Figure 3

CHAPTER 6. CONCLUSIONS

The work in this dissertation has described the development of two applications of laser-induced fluorescence detection, the development of high-throughput screening technique for heterogeneous catalysts by laser-induced fluorescence imaging and single cells analysis by LIFI-CE. The screening technique was used in combinatorial discovery of active catalysts for oxidation of naphthalene, some combinations have demonstrated up to 70% higher catalytic activity than conventional catalysts, vanadium pentoxide. In study unstable zeolite catalytic system, LIFI provided an efficient way to optimize the catalytic process as well the regeneration of deactivated zeolites. The screening throughput for heterogeneous catalysts has been significantly improved by LIFI, the activity mapping for a combinatorial library can be obtained in less than 10s, which can't not be done either by conventional approach or other high-throughput screening techniques.

In this work, although we demonstrated the application of LIFI mostly on a 15-membered library, a larger library can be easily adopted by some minor modification of optics and reactor size. For the future efforts, it is interesting to couple this high-throughput screening technique with a suitable combinatorial synthesis technique that can provide a larger member library. Application of LIFI screening for larger libraries should be more impressive and usefult. Also, more efforts should be devoted to the applications of this technique in various catalytic systems.

APPENDIX. SUPPORTING INFORMATION

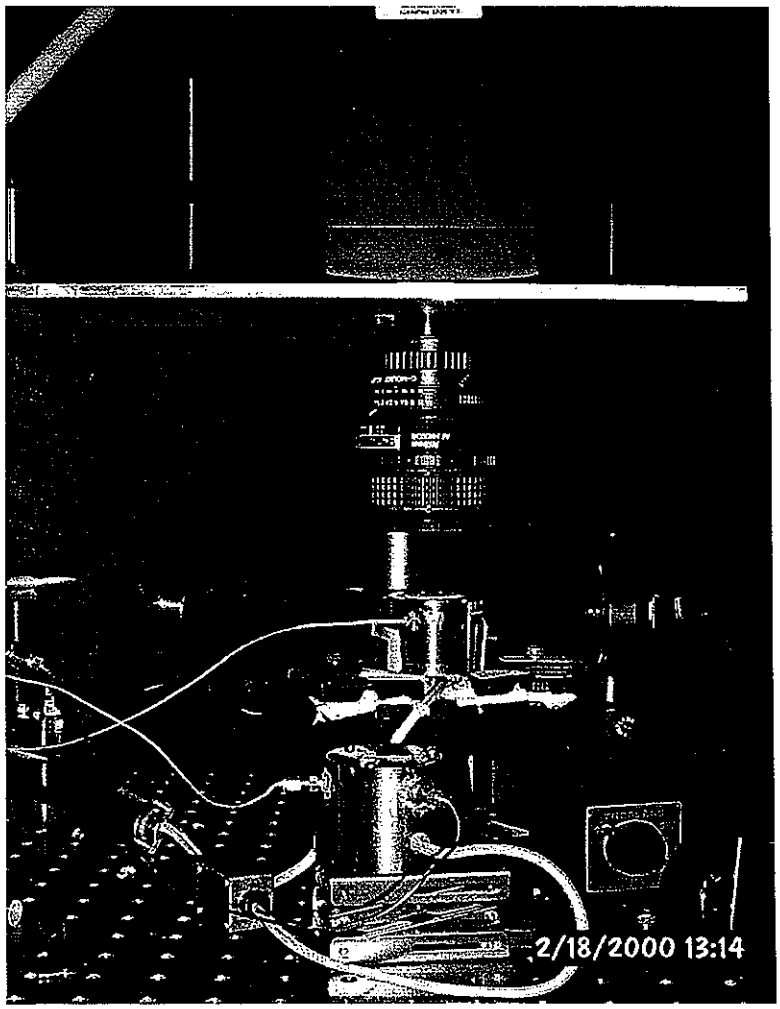

Figure 1. Instrumentation

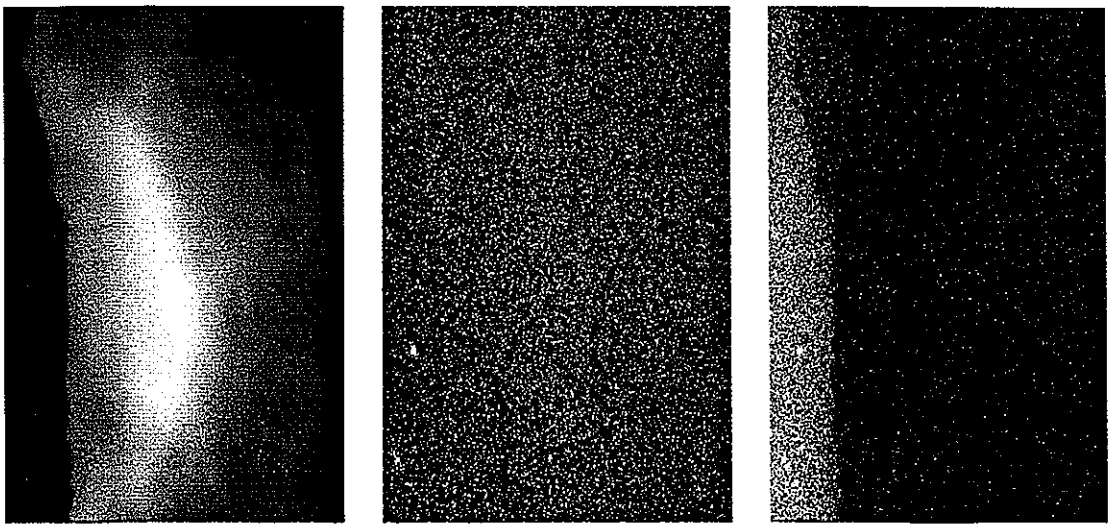

b

Figure 2. a. Optical image of V2O5 pellet, left darker part of the image. Reactants flow from left to right b. Fluorescence image when no reactants introduced into reactor. c. Fluorescence image after reactant was introduced into the reactor.

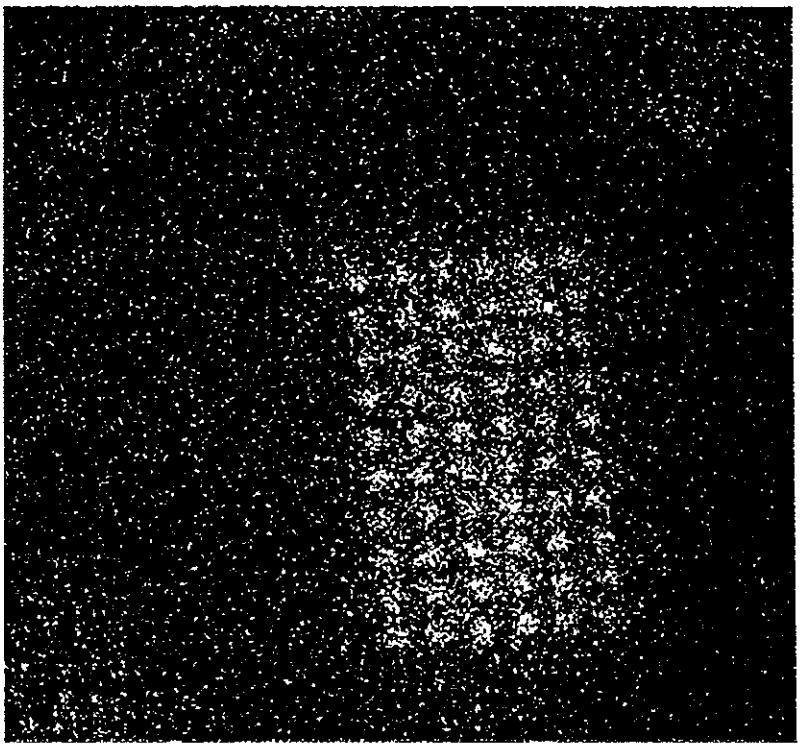

Figure 3. LIFI screening for a 60-membered library

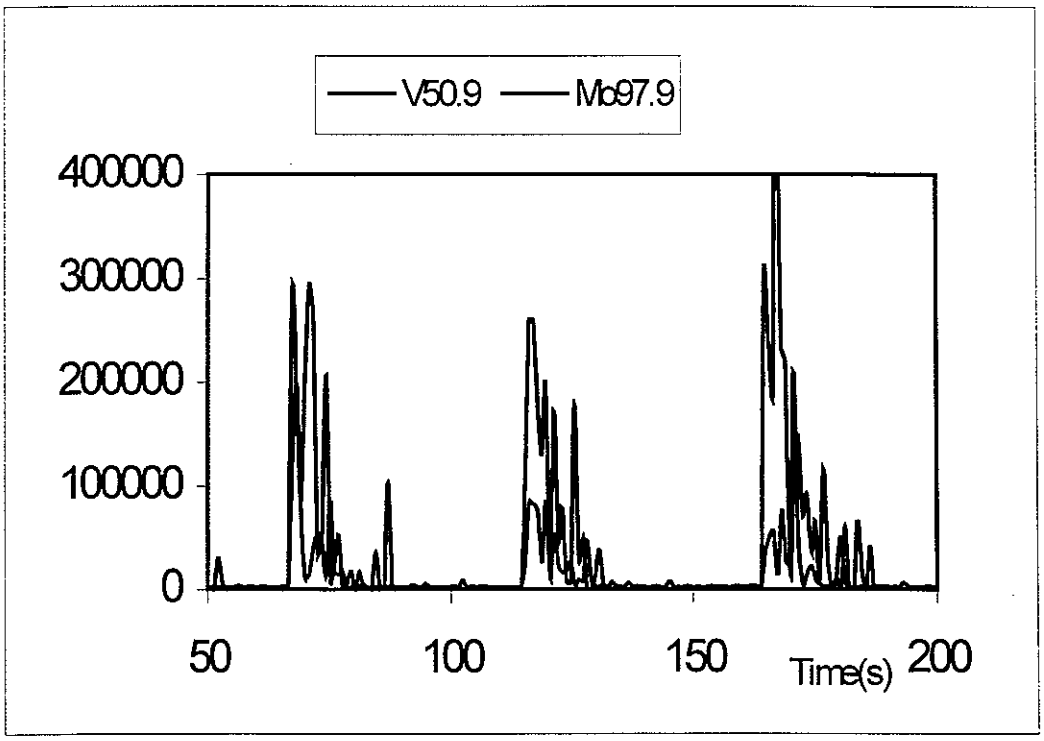

Figure 4. ICP-MS Spectrum for Mo_V(A), Mo/V=7/3

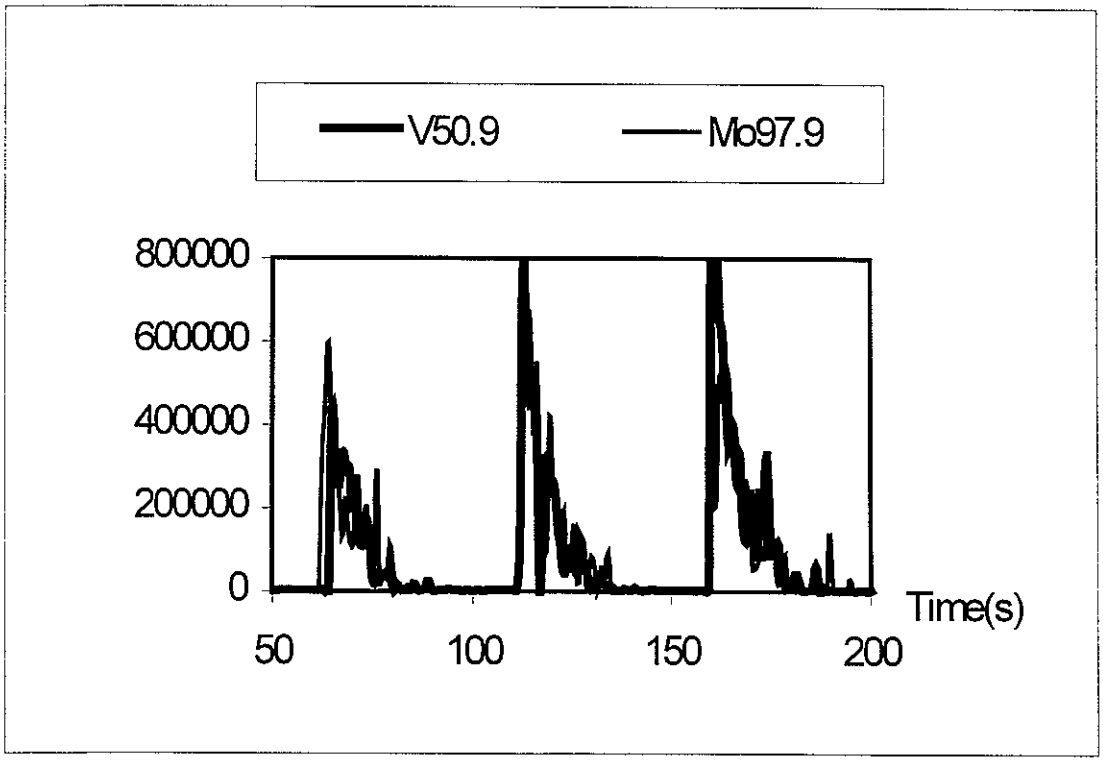

Figure 5. ICP-MS spectrum for Mo_V(A), Mo/V=1

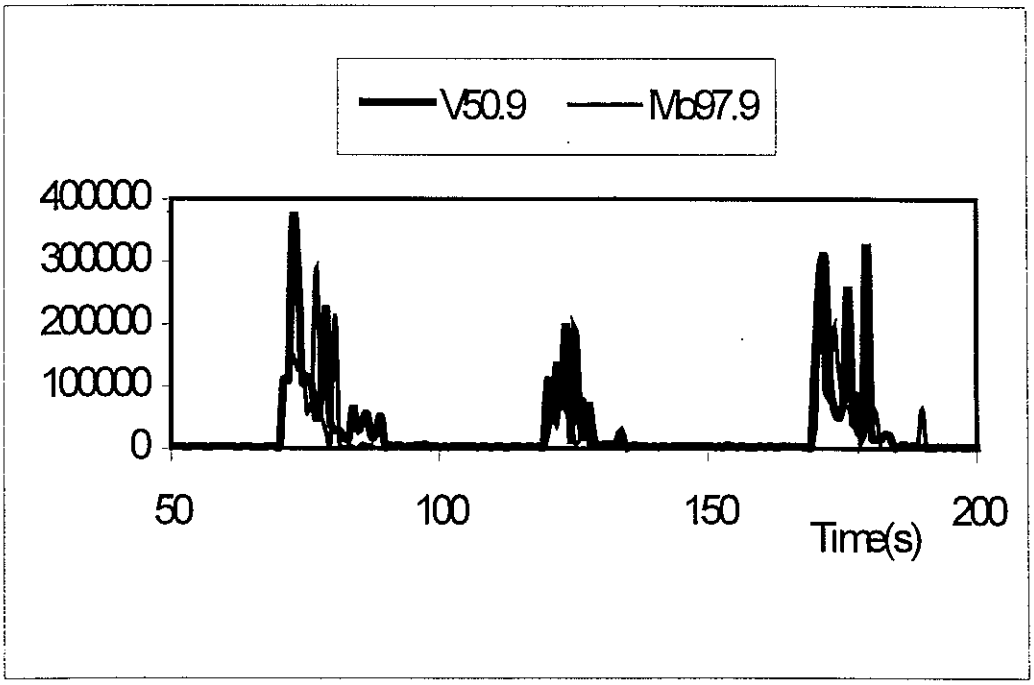

Figure 6. ICP-MS Spectrum for Mo_V(A), Mo/V=3/7

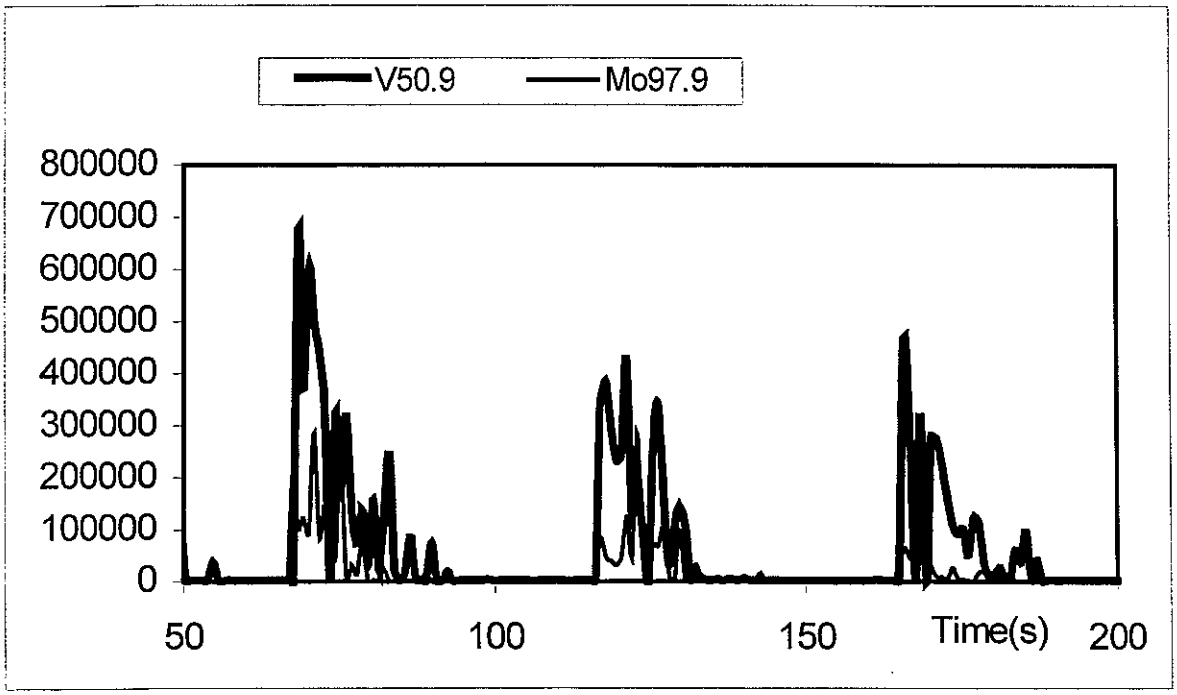

Figure 7. CP-MS Spectrum for Mo_V(A), Mo/V=1/9

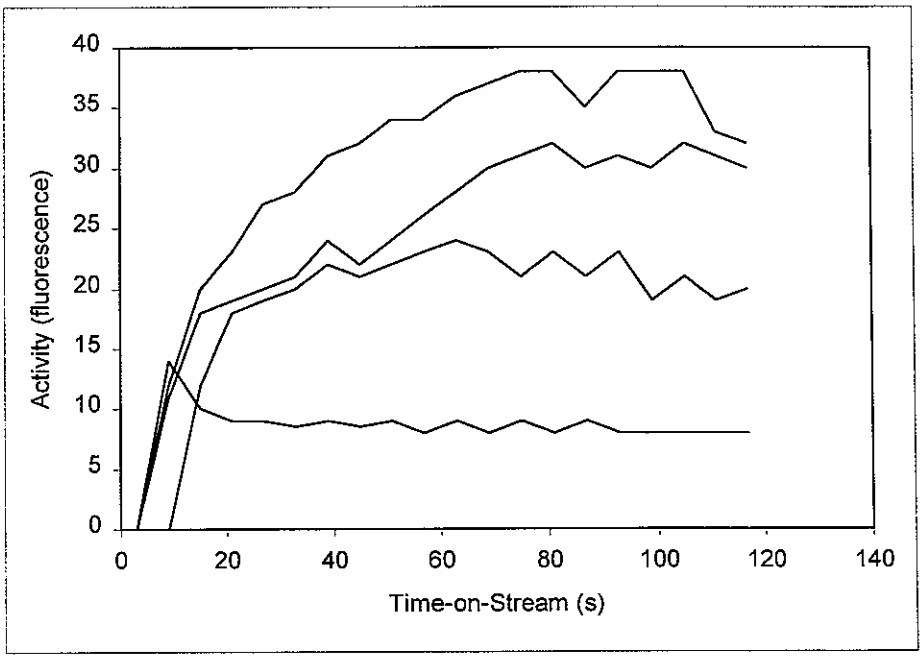

Figure 8. Catalytic Properties of Beta Zeolite of Si/Al=25

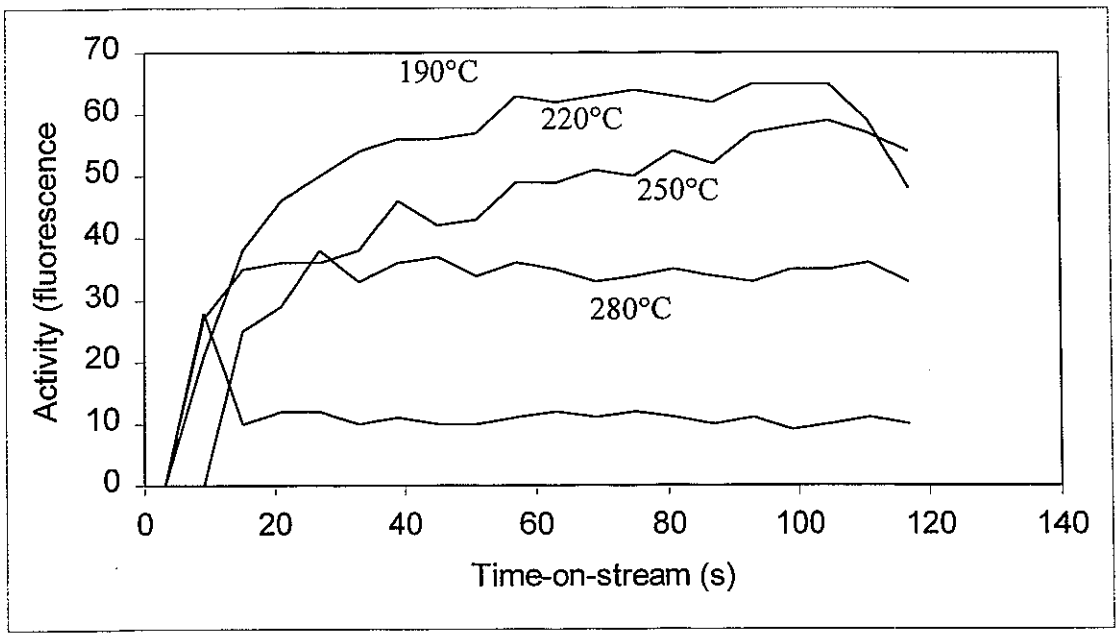

Figure 9. Catalytic Properties of Beta Zeolite of Si/Al=75

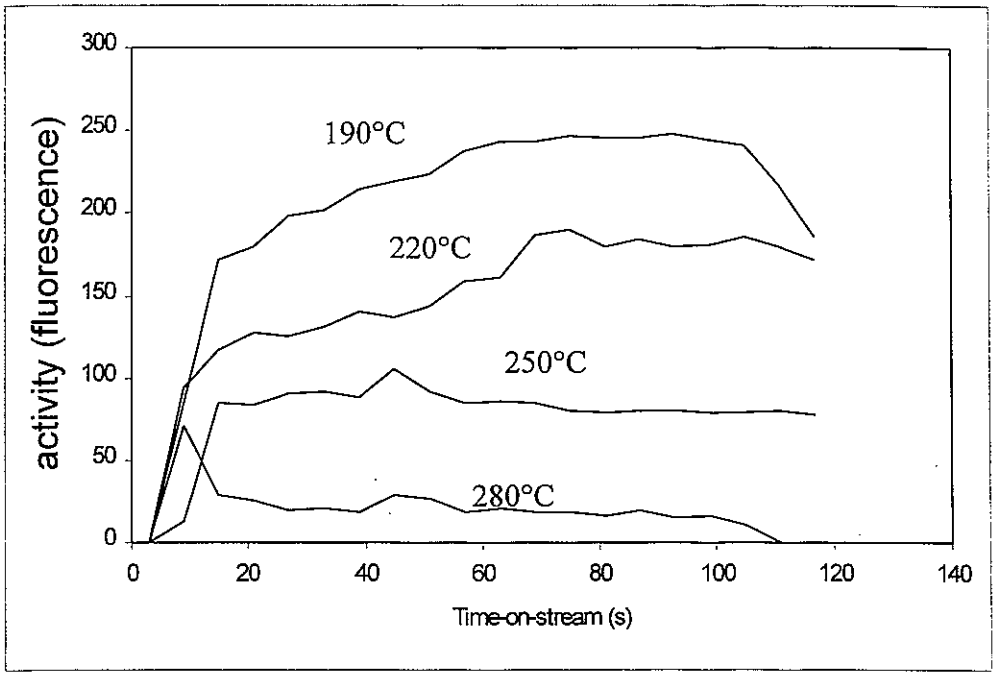

Figure 10. Catalytic Properties of Beta Zeolite of Si/Al=150

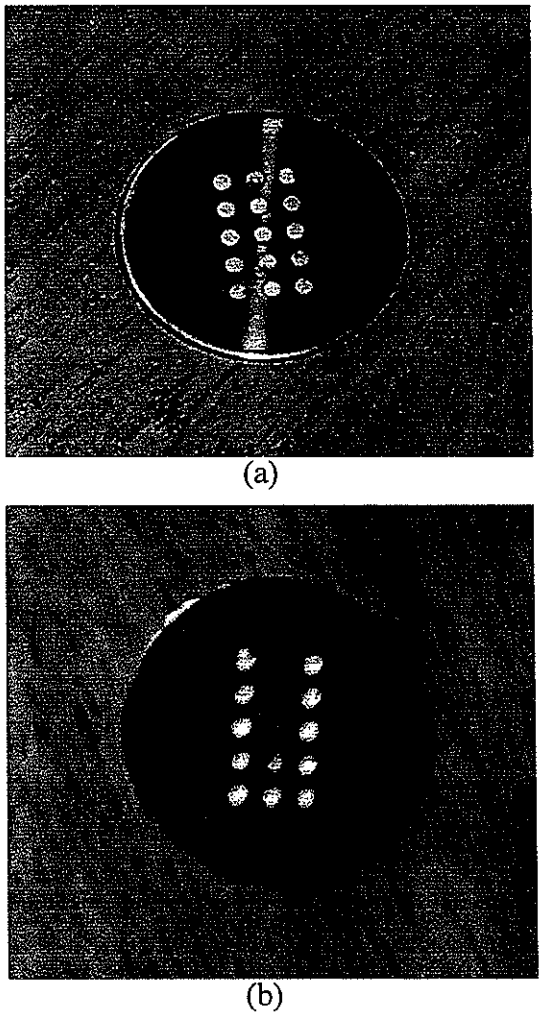

Figure 11 zeolite library (a) before reaction and (b) after reaction

ACKNOWLEDGMENTS

First of all, I would like to express my sincere gratitude towards my major advisor, Professor Edward S. Yeung. I thank him for his encouragement, understanding and patience during my graduate study. Dr. Yeung is such a devoted scientist and I am so glad to a member of his research team.

I would also like to thank my committee members, Dr. Beitz, Dr. Houk, Dr. Johnson, Dr. Graves and Dr. Thiel for their time and encouragement.

I would like to express my appreciation to Dr. Houk and his graduate student, Yongjin Hou, Dr. Schrader and his graduate students for their cooperation and help in this work.

Thanks all the past and present members of the yeung's group with whom I have worked. Especially to Andrea Ho, Dr. Hongdong Tan, Dr. Nanyan Zhang, Dr. Xiaoyi Gong, Dr. Yonghua Zhang, Dr. Wei Wei, Hanlin Li, Gong Xue, Mike Christolulu. I really appreciate their help and friendship.

To my aunt Li and uncle Xue, I could never acknowledge all that they have done for me. They brought me up and have been there for me every single step in life, loving me, supporting me, and sharing my happiness and struggles. I own my whole life to them.

Thank my parents for bringing me to this world.

I would also like to thank my husband Yimin for supporting me during my graduate study.